Graphing, Interpretation, and Comparison of Results of Loudspeaker Nonlinear Distortion Measurements*

ALEXANDER VOISHVILLO, *AES Member,* **ALEXANDER TEREKHOV, EUGENE CZERWINSKI, AND SERGEI ALEXANDROV****

Cerwinski Laboratories Inc., Simi Valley, CA 93063, USA

Harmonic distortion and total harmonic distortion may not convey sufficient information about nonlinearity in loudspeakers and horn drivers to judge their perceptual acceptability. Multitone stimuli and Gaussian noise produce a more informative nonlinear response. The reaction to Gaussian noise can be transformed into coherence or incoherence functions. These functions provide information about nonlinearity in the form of "easy-to-grasp" frequency-dependent curves. Alternatively, a multitone stimulus generates a variety of "visible" harmonic and intermodulation spectral components. If the number of input tones is significant, the nonlinear reaction may consist of hundreds, if not thousands, of distortion spectral components. The results of such measurements are difficult to interpret, compare, and overlay. A new method of depicting the results of multitone measurements has been developed. The measurement result is a single, continuous, frequency-dependent curve that takes into account the level of the distortion products and their "density." The curves can be easily overlaid and compared. Future developments of this new method may lead to a correlation between curves of the level of distortion and the audibility of nonlinear distortion. Using nonlinear dynamic loudspeaker models, multitone and Gaussian noise test signals are compared with traditional and nontraditional measurement techniques. The relationship between harmonics and intermodulation products in static and dynamic nonlinear systems is analyzed.

0 INTRODUCTION

Loudspeakers and horn drivers are complex nonlinear dynamic systems whose nonlinear reactions to different stimuli may be significantly different. It has been demonstrated earlier that traditional methods of measuring nonlinear distortion using a sweeping tone, and such criteria as harmonic distortion and total harmonic distortion (THD), may not convey sufficient information about the nonlinear properties of loudspeakers and horn drivers [1]. It has been demonstrated by using the multitone stimuli that the intermodulation products outweigh the harmonics in even comparatively simple nonlinear systems characterized by static polynomial nonlinearity. This difference between harmonics and intermodulation products is especially pronounced if a higher order nonlinearity occurs. In complex nonlinear dynamic systems, such as electrodynamic direct-radiating loudspeakers or horn drivers, the intermodulation and harmonic products are characterized by their individual dependence on frequency. These individual dependencies prevent a substitution of intermodulation testing with harmonic measurements.

Complex signals such as multitone stimuli and Gaussian noise produce nonlinear reactions that carry more information about intermodulation of various kinds and orders in loudspeakers and horn drivers. Nonlinear reactions to the Gaussian noise can be transformed into, for example, the Wiener kernels [2], coherence or incoherence functions [3], [4], or the higher order spectra (HOS) [5]. Wiener kernels do not have an intuitive simple interpretation. The coherence (or incoherence) functions and HOS provide information about the overall nonlinear behavior of a measured object in the form of "easy-to-grasp" frequency-dependent curves. However, these functions are also sensitive to noises and other effects (such as reflections) that may "mar up" the results of nonlinear testing. In addition, it takes a comparatively long time to measure them. Historically the coherence function has been used in the testing of hearing aids [3], [4] and in the evaluation of nonlinearity and noises in magnetic recording [6], but has

*Manuscript received 2002 May 9; revised 2003 December 12 and 2004 February 13.

**Now with JBL Professional, Northridge, CA 91329, USA.

never been popular in the assessment of loudspeaker nonlinearity. The multitone stimulus has been gaining popularity in many applications during the last decade [7]–[12]. Various aspects of using multitone signals in loudspeaker testing will be discussed in Section 3. The multitone stimulus produces a rich spectrum of distortion products. The statistical distribution and crest factor of multitone signals is close to that of a musical signal. However, the results of a measurement presented in the form of an output spectrum are difficult to interpret, compare, and overlay.

A new method of depicting the results of multitone measurements has been developed in this work. According to this method, the result of the measurement is presented as a single, continuous, frequency-dependent curve that takes into account not only the distortion level of the spectral components but also their "density." Many such curves, corresponding to different levels of input signal, can be overlaid easily in a way that is practically impossible using "unprocessed" responses to the multitone stimulus. These two- or three-dimensional graphs can easily demonstrate how the overall nonlinear distortion in a device measured (loudspeaker or horn driver) increases with the level of the input multitone stimulus.

In the technical publications of previous years other approaches to measure, model, and assess loudspeaker nonlinearity have been discussed. Some of these methods have not been included in the existing standards and probably never will. However, a comparative survey helps us to look at the problem of loudspeaker nonlinearity measurements from a systematic standpoint and to understand better their meaning, advantages, and limitations. The traditional and nontraditional methods that will be compared to the methods based on the application of Gaussian noise (incoherence function) and multitone stimulus are reviewed hereafter.

One of the unconventional methods is the measurement and graphing of high-order frequency response functions (HFRFs) derived from the second- and third-order Volterra time-domain kernels. The HFRFs are three-dimensional graphs, representing a "surface" of distortion products. Volterra series expansion stems from the fundamental theoretical input of Volterra [13] and has been introduced by Wiener for the analysis of weakly nonlinear systems, characterized by low levels of distortion (see [14] for a history of this subject). Since then Volterra series expansion has been used widely in many areas where the structure of weakly nonlinear systems is not known, or the parametric analysis of their behavior is too complicated. Kaizer pioneered the use of Volterra series in loudspeaker nonlinear analysis. He derived explicit expressions for HFRFs through loudspeaker excursion-dependent parameters [15]. Kaizer's research was followed by a number of works (for example, [16]–[18]), where the second- and third-order kernels were measured, transformed into corresponding HFRFs, and then plotted as three-dimensional graphs depicting loudspeaker second- and third-order distortions. Advantages and drawbacks of Volterra series expansion will be discussed in the Section 3.

Two-tone intermodulation distortion of the second and third order has traditionally been measured to assess nonlinearity in audio equipment since two methods were introduced in the 1940s by Hilliard [19] (SMPTE intermodulation distortion) and Scott [20] (difference-frequency or CCIF distortion). The former uses one sweeping and one stationary low-frequency tone of four times higher amplitude. The latter method uses two closely spaced simultaneously swept tones. Products of the kind $P_{f_2 \pm f_1}$ and $P_{f_2 \pm 2f_1}$ are plotted. The frequency f_1 corresponds to the fixed tone in the SMPTE method or to the lower frequency tone in the CCIF method, and f_2 is the frequency of the higher sweeping tone. Both methods do not measure intermodulation products of order higher than three.

For the measurement of loudspeaker nonlinearity AES standard AES2-1984 [21] recommends a measurement of only the second- and third-order harmonic distortion. IEC standard 60268-5 [22] recommends that a wider circle of characteristics be measured, including THD, individual second and third harmonics, and individual second-order difference intermodulation products. In addition this standard recommends the aggregated criteria of sound pressure level (SPL) intermodulation in the form $(P_{f_2+f_1} + P_{f_2-f_1})/P_{f_2}$ and $(P_{f_2+2f_1} + P_{f_2-2f_1})/P_{f_2}, f_2 >> f_1$, where the sum and difference products of similar order (second or third only) are summed and related to one of two primary tones.

Alternative approaches to measure loudspeaker intermodulation distortion were proposed by Keele [23]. Keele recommends two methods for consideration, one based on the use of two-tonal signals, 40 and 400 Hz, of equal amplitude. The percent of distortion is to be plotted as a function of input power. The other method includes a fixed-frequency upper range signal coupled with a swept bass signal. Keele also advocates the use of the shaped tone burst for the assessment of loudspeaker maximum SPL [24].

These various methods and signals provide different information about the nonlinearity in a measured loudspeaker. Nevertheless, the following questions remain open: "What method conveys most adequate information about nonlinearity in a measured loudspeaker?", "How well are the measurement data related to the perceived deterioration of sound quality or to the malfunctioning of a loudspeaker?", and "How can these data be represented in the most comprehensible manner?".

This work is intended to illustrate and compare several methods of assessment and graphical presentation of weak nonlinearity in loudspeakers. The comparison is carried out using a nonlinear dynamic model of a low-frequency loudspeaker that includes excursion-dependent parameters: *Bl* product, suspension stiffness, voice-coil inductance, parainductance, eddy currents–caused resistance, and voice-coil current-dependent magnetic flux modulation. The models of three different woofers are used for comparison: 8-in (203-mm) diaphragm long voice coil, 8-in (203-mm) diaphragm short voice coil, and 12-in (305-mm) diaphragm long voice coil. The measurement results are simulated at different signal levels. A comparison is made of THD, harmonic distortion, Volterra second-order frequency-domain kernels, also called high-order frequency response functions (HOFRF), two-tone sum and difference intermodulation distortion, two-tone total non-

linear distortion, multitone intermodulation and multitone total nonlinear distortion (MTND), and incoherence function.

1 TEST SUBJECT, TEST RESULT PRESENTATION, AND GOAL

The possible uncertainty in the objective assessment of nonlinear systems by traditional testing methods stems from the complex nature of nonlinear systems. A linear time-invariant system with a single input and output is fully described by its pulse response (or by its complex transfer function). The output signal can be calculated by the convolution of the input signal with the impulse response (in the time domain), or by multiplication of the input spectra by the complex transfer function (in the frequency domain). In addition, the relationship between an input and an output signal of a linear system can also be expressed in the form of a linear differential equation or a linear difference equation if a linear system is discrete. Simply speaking, a linear system does not add new frequency components to the output signal.

The behavior of a nonlinear system is substantially more complex. Traditional methods used for the analysis of linear systems are not applicable for an analysis of even weakly nonlinear systems. The properties of such systems can be described in the time domain by the sum of Volterra kernels [14]. The latter are essentially the pulse responses responsible for the transformation of input signal by nonlinearities of different orders. The overall pulse response of a weakly nonlinear system is the sum of kernels of different orders that are multidimensional functions of time. For example, the pulse response of a simple nonlinear system characterized by a second-order dynamic weak nonlinearity is the sum of the kernels of the first order (which is essentially the linear pulse response) and a second-order kernel. The latter can be presented graphically as a three-dimensional surface with two horizontal time scales.

The output of such a system can be expressed as the convolution of an input signal with the first- and second-order kernels. This convolution is expressed in general by multiple integrals. The multidimensionality is also valid for a frequency-domain complex transfer function of nonlinear systems. The amplitude and phase frequency responses of a second-order distortion are also three-dimensional surfaces having two horizontal frequency scales. The second harmonic distortion response (amplitude and phase) is merely a diagonal "cut" through these two surfaces. Similarly, the impulse response of the second harmonic is merely a diagonal cut across the surface of the three-dimensional kernel of the second order [1]. It is obvious that neither the frequency response of the second harmonic nor its impulse response will represent the entire second-order nonlinear response of a weakly nonlinear dynamic system legitimately. These cuts may not correspond to the maxima of the distortion surface. Using only harmonic distortion may cause mistakes in the assessment of the nonlinearity. Therefore a search for a correlation between the audibility of nonlinearly distorted musical signals and the level of harmonic distortion can lead to wrong conclusions. The present example considers the three-dimensional representation of the second-order nonlinearity. The responses of the higher order nonlinearities are multidimensional functions. A real dynamic nonlinearity existing in loudspeakers and horn drivers is significantly more complex than this simple example.

Imagine a hypothetical loudspeaker whose amplitude frequency response is presented by only a few samples at a few frequencies. If there is no information about the behavior of the amplitude frequency response between these sparse samples, we cannot make a judgment about its performance. The response of this loudspeaker might be perfectly flat between available samples; it might as well have a strong irregularity. Similarly, a single frequency response of nonlinear distortion, be it a harmonic or an intermodulation curve, conveys only limited information about the nonlinearity. If there is no information about a surface of nonlinear responses between the available cuts of harmonic or intermodulation frequency responses, the behavior of the nonlinear system cannot be assessed accurately. This statement is valid for loudspeakers and horn drivers, which are complex, dynamic nonlinear systems with many degrees of freedom and whose nonlinear responses depend strongly, and in a complex manner, on the frequency. In amplifiers, for example, the nonlinear characteristics do not exhibit that strong a frequency dependence. Therefore, in their analysis the relationship between harmonic and intermodulation distortions might be more predictable.

The examples with nonlinear distortion in the loudspeakers described in this work will assume weak nonlinearity (distortion products are at least 20–30 dB lower than the fundamental signal). In reality, however, the distortion in loudspeakers and horn drivers can be higher, placing loudspeakers and drivers in the category of strongly nonlinear systems. These systems are characterized by even more sophisticated properties that may include bifurcation and chaotic and stochastic behavior. This class of nonlinear systems will not be considered in the current work.

There is a dilemma in measuring, graphing, and interpreting nonlinear distortion. On the one hand the assessment of nonlinear distortion needs the analysis of much more information than is required to assess a linear system. On the other hand this information should be presented in a simple and comprehensible graphical manner. These two requirements may contradict each other. Furthermore, the graphed data should be pertinent from the standpoint of distortion audibility. The final goal of a loudspeaker nonlinear distortion measurement is to obtain data that convey adequate information about the nonlinearity so that this information can be related unambiguously to the perceived sound quality of a loudspeaker under test, and that thus the performance of different loudspeakers can be compared objectively. The measurement data must be "manageable." In spite of the seeming simplicity of these goals, and a nearly 90-year history of numerous efforts of many researchers (see [1] for a history of the subject), these goals have never been fully achieved.

2 PSYCHOACOUSTICAL CONSIDERATIONS

The search for a correlation between an objective measurement of nonlinear distortion and the subjective audibility of nonlinear distortion in audio equipment in general, and in loudspeakers in particular, has always been and remains the Holy Grail of the audio industry. Loudspeaker distortion measurement data related to the perceived sound quality must not only have some readily comprehensible interpretation, but must also be supported psychoacoustically. There must be a credible knowledge relating the graphically presented objective data to the subjectively perceived sound quality. Due to the complex nature of the nonlinearity and the intricacy of the human auditory system's reaction to a musical signal adversely affected by the nonlinearity, there are no undisputedly credible and commonly recognized thresholds expressed in terms of the traditional nonlinear distortion measures related to the perceived sound quality. The problem is aggravated by the fact that the objective measurement of nonlinearity deals merely with the symptoms of a nonlinear system, that is, with the reactions of a nonlinear system, such as a loudspeaker, to various testing signals. Here we operate with objective categories, such as measured levels, responses, characteristics, and parameters. Meanwhile the subjective assessment of musical signals impaired by the nonlinearity deals with the human psychoacoustical reactions and impressions expressed in a quite different vernacular, such as "acceptable, annoying, pleasant, or irritating." The objective of a researcher is to put a bridge between these two different domains.

The dynamic reaction of a complex nonlinear system (such as a direct-radiating loudspeaker or a horn driver) to a musical signal cannot be extrapolated from its reaction to a simple testing signal such as a mere sweeping tone. Hence the credible thresholds of subjectively perceived nonlinear distortion expressed in terms of the reaction to simple sinusoidal signals (THD, harmonics, or two-tone intermodulation distortion) may not be valid. More complex signals, such as a random or pseudorandom noise or a multitone stimulus, are believed (by the authors) to be required to search for subjectively relevant thresholds.

The complex properties of the human hearing system, which is a far cry from a mere Fourier frequency analyzer, only add complexity to the problem. The behavior of the hearing system is characterized by many effects described in various publications on psychoacoustics (see [25], for example). The properties of the auditory system most relevant to the subject of this work are the intrinsic nonlinearity of the hearing system and temporal and frequency-domain masking. These effects have been treated in detail in the psychoacoustical literature, and it is not the authors' goal to replicate these texts. However, it is worth mentioning that the intrinsic nonlinearity of the human hearing system manifests itself at high levels of sound pressure, whereas the masking is a general property of the hearing system, "working" at any level of the sound pressure signal.

The masking plays a crucial role in the perception of nonlinear distortion. The crux of masking is a psychoacoustical suppression of a weaker masked signal by a stronger signal, called masker. The masking may be observed in the time domain in the form of post and premasking when a stronger short-term masker "obliterates" a weaker masked signal, even if the latter precedes the masker. Masking may also occur in the frequency domain, where a stronger masker produces a shadow zone around itself. This shadow psychoacoustically suppresses those masked signals whose spectrum components happen to be within the spectrum and below the level of the masking frequency-domain curve. The masking frequency-domain curve produced by a single tone, for example, resembles a triangle. With an increase in the level of the masker, the triangle becomes asymmetrical, with its longer side stretching toward high frequencies [25]. With an increase in the level of the masking tone the level of the masking asymmetrical triangle increases and stretches over a wider frequency range, producing a stronger masking effect above the frequency of the sinusoidal masker rather than below it (Fig. 1). The masker shown in Fig. 1 corresponds to curve a.

The asymmetrical triangular shape of the masking curve explains why the higher order harmonics and intermodulation products are more audible than the lower order ones, who are more prone to be masked. In Fig. 2 the harmonics and intermodulation products, produced by a two-tone signal affected by the static fifth-order nonlinearity, are overlaid with the masking curve produced by the two-tone masker. This also explains why the difference intermodu-

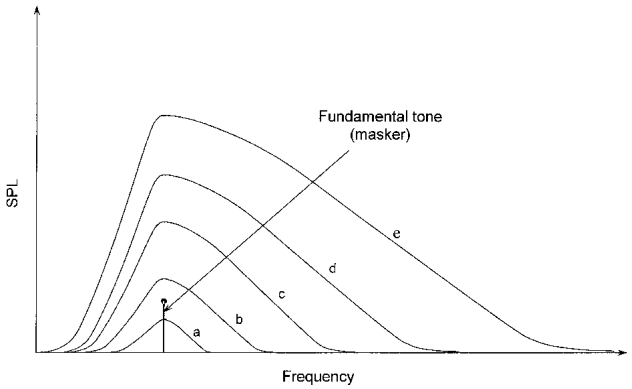

Fig. 1. Masking curves corresponding to levels a–e of sinusoidal tone masker. The masker corresponds to curve a.

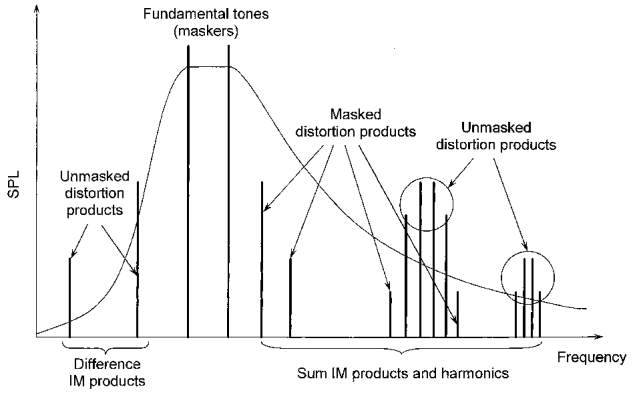

Fig. 2. Masking effects produced by two closely spaced fundamental tones (maskers) on their harmonics and intermodulation products.

lation products are more susceptible to be outside the narrower lower side of the masking curve, which makes them more audible. In addition, the frequencies of the harmonics have a higher probability of coinciding with overtones of particular musical instruments, and of being masked by these overtones as well. Meanwhile the variety of "dissonant" intermodulation products of various orders do not coincide with the overtones of the musical instruments and, therefore, are more noticeable.

The complexity of nonlinear systems such as loudspeakers and the complexity of the hearing system explain why thresholds of distortion audibility expressed in terms of such plain metrics as harmonic distortion, THD, and two-tone intermodulation distortion strongly depend on the type of musical signal used in the experiments, and why the data obtained by different researchers are often inconsistent. An historical review of the search for a relationship between objective data (expressed in terms of such metrics as THD, harmonic distortion, and two-tone intermodulation distortion) and the subjectively perceived deterioration of the sound quality of reproduced material is given in [1]. Historically many early research works in this area did not have a clear understanding of the complex nature of nonlinear dynamic systems and suffered from a lack of the modern knowledge of the principles of operation of the hearing system. Since then the theory of nonlinear systems and the knowledge of psychoacoustics have progressed enormously. Examples of the use of this progress are the systems of low-bit compression (such as MP3, WMA, ATRAC) that "deceive" the hearing system by deleting significant parts of signal information without a significant deterioration of the perceived sound quality. These low-bit-rate compression systems, evaluated by standard metrics such as THD or two-tone intermodulation distortion, would have exhibited unacceptable levels of distortion, proving that the standard metrics have no immediate relationship with the perceived sound quality.

Continuing this line of thought, THD, which is the most popular measure of nonlinear distortion in audio, is not a reliable measure of the psychoacoustically meaningful nonlinearity in a loudspeaker. First, it does not add anything to what individual harmonic curves can show. Second, since useful information about harmonics of different orders is not available from THD, its interpretation may result in wrong conclusions about the character of the nonlinearity in a loudspeaker tested. In other words, the same 10% THD of the sound pressure level at a certain level of input voltage might be produced by the dominant second- and third-order nonlinearities in one loudspeaker, or it might include the higher order harmonics in another loudspeaker as well. The difference in the amount and level of intermodulation products and, correspondingly, in the sound quality of these two loudspeakers could be significant. This THD would not indicate.

As has been mentioned, the multitone stimulus, whose objective parameters, such as the probability density function, have similarity with a musical signal, seems to be a good candidate for a better testing signal. However, there is an important aspect of using multitone stimuli that should be considered here to be objective. Currently the interpretation of multitone test results does not have a well substantiated psychoacoustical support. So far we cannot derive precise judgments about the sound quality of a loudspeaker (that has been tested by a multitone stimulus) from the response to this signal. However, the results of recent research on the correlation between objective measurements and subjectively perceived nonlinearly distorted speech and musical signals [26] prove that for certain kinds of nonlinearity the postprocessed reaction to a multitone stimulus expressed as a single number, dubbed by the authors of that work the distortion score (DS), has a very high correlation with subjectively perceived sound quality. The distortion score is obtained by the summation of the levels of distortion products within the mean equivalent rectangular bandwidth (ERB_N) of the auditory filter, which is conceptually similar to the traditional critical bandwidth but differs in numerical values. It is believed that future experiments with multitone stimuli might lead to further positive results in attempts to find a relationship between the objective measurement data and subjectively perceived sound quality.

3 TESTING METHODS AND INTERPRETATION OF MEASUREMENT DATA

3.1 Relationship between Harmonics and Intermodulation Products—Effects Produced by Static Nonlinearity of Different Orders

Measurements of nonlinear distortion using simple excitation signals may not provide adequate information about the nonlinear properties of a device under test. Even considering a simple form of static nonlinearity, some not immediately obvious effects appear. Let a hypothetical static nonlinear system be governed by the simple polynomial expression

$$y(t) = \sum_{i=0}^{n} h_i z^i(t) \tag{1}$$

where $z(t)$ is an input signal, $y(t)$ is an output signal, h_0 is the dc distortion component, h_1 is the linear gain coefficient, and $h_2, \ldots, h_n$ are the weighting coefficients responsible for the influence of a nonlinearity of a particular order beginning from the second. The coefficients h_i in general may have positive or negative signs, and some of them may be zero.

A nonlinearity of this kind might, for example, approximate a loudspeaker suspension in the form of a relationship between the diaphragm displacement x and the force F if creep effect (the long-term dependence of the compliance on the time of loading) and hysteresis are omitted. Then the coefficients $h_0, \ldots, h_n$ in Eq. (1) represent the suspension compliance. As a loudspeaker operates, nonlinear compliance causes nonlinear displacement, and this effect interacts with other nonlinear phenomena. The overall nonlinearity of loudspeakers is dynamic and more complex than the simple relationship described by Eq. (1). Bearing in mind that this particular example is not a complete representation of the operation of a loudspeaker, we will nevertheless analyze this simple static nonlinearity to illustrate some general effects.

Let us assume that the relationship between the displacement, x (output) and the force F (input) is described by the expression: $x(t) = c_1F(t) - c_5F^5(t)$, where the coefficients c_1 and $-c_5$ represent nonlinear mechanical compliance. We also assume that the input driving force is sinusoidal and the coefficient c_5 is set to $c_5 = 0.26344$ to produce 10% THD in displacement. Fig. 3 shows the dependence of the displacement on the driving force and the spectrum of displacement corresponding to the sinusoidal input. The spectral components of displacement are described by the expression

$$\begin{aligned} x(t) &= c_1F \sin \omega t - c_5F^5 \sin^5 \omega t \\ &= c_1F \sin \omega t - c_5F^5(0.625 \sin \omega t - 0.3125 \sin 3\omega t \\ &\quad + 0.0625 \sin 5\omega t). \end{aligned} \tag{2}$$

The fifth-order "limiting" nonlinearity produces the fifth harmonic (which is quite predictable). It also generates the third harmonic and the spectral component having the same frequency as the input signal. Since the latter spectral component is out of phase with the fundamental tone it produces the limiting effect of the suspension because it decreases the level of the first harmonic in the displacement compared to the linear one. The fifth harmonic is five times (−14 dB) smaller than the third and ten times (−20 dB) smaller that the spectral component having the same frequency as the input tone.

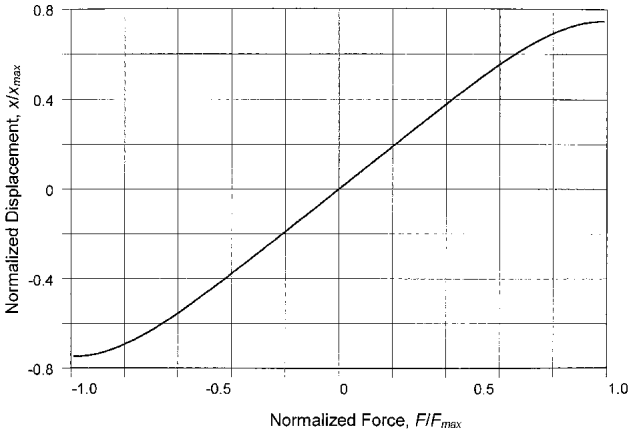

(a)

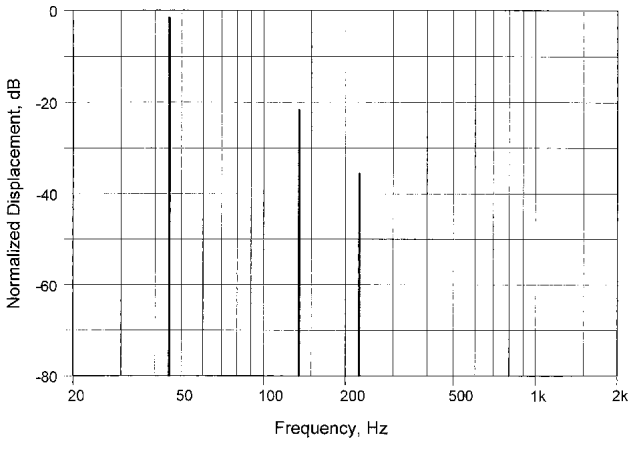

(b)

Fig. 3. (a) Dependence of suspension displacement on force; fifth-order approximation. (b) Spectrum of displacement corresponding to fifth-order approximation. Sinusoidal input.

If the input force F has the form of a two-tone signal, $F \cdot 0.5(\sin \omega_1 t + \sin \omega_2 t)$, then the output signal (displacement) consists of the linear part $c_1F \cdot 0.5(\sin \omega_1 t + \sin \omega_2 t)$ and of the distortion products generated by the fifth-order nonlinearity, which include two fifth and two third harmonics, and twelve intermodulation products. In addition, the fifth-order nonlinearity produces two spectral components having frequencies identical to the frequencies of the initial input signals. Fig. 4 depicts the output spectrum. We assume that the amplitude of each tone is half the amplitude of the previous sinusoidal tone to maintain the same maximum level as the single-tone signal,

$$\begin{aligned} x(t) &= c_1F \cdot 0.5(\sin \omega_1 t + \sin \omega_2 t) \\ &\quad - c_5F^5 \cdot 0.5^5(\sin \omega_1 t + \sin \omega_2 t)^5 \\ &= c_1F \cdot 0.5(\sin \omega_1 t + \sin \omega_2 t) \\ &\quad - c_5F^5 \cdot 0.03125[0.0625 \sin 5\omega_1 t \\ &\quad + 0.0625 \sin 5\omega_2 t - 1.5625 \sin 3\omega_1 t \\ &\quad - 1.5625 \sin 3\omega_2 t + 6.25 \sin \omega_1 t + 6.25 \sin \omega_2 t \\ &\quad - 3.125 \sin (2\omega_1 + \omega_2)t + 3.125 \sin (2\omega_1 - \omega_2)t \\ &\quad - 3.125 \sin (2\omega_2 + \omega_1)t + 3.125 \sin (2\omega_2 - \omega_1)t \\ &\quad + 0.3125 \sin (4\omega_1 + \omega_2)t - 0.3125 \sin (4\omega_1 - \omega_2)t \\ &\quad + 0.3125 \sin (4\omega_2 + \omega_1)t - 0.3125 \sin (4\omega_2 - \omega_1)t \\ &\quad + 0.625 \sin (3\omega_1 + 2\omega_2)t + 0.625 \sin (3\omega_1 - 2\omega_2)t \\ &\quad + 0.625 \sin (3\omega_2 + 2\omega_1)t + 0.625 \sin (3\omega_2 - 2\omega_1)t]. \end{aligned} \tag{3}$$

The balance between fifth and third harmonics becomes significantly different compared to the single-tone excitation. The fifth harmonic turns out to be much lower in amplitude than the third harmonic and all intermodulation products. The difference between the fifth and third harmonics produced by the same fifth-order nonlinearity becomes 28 dB. All twelve intermodulation products are higher in amplitude than the fifth harmonic. If the maximum level of the two-tone signal is chosen equal to the amplitude of the single-tone signal producing 10% THD, the relationship between the harmonics produced by these two signals is as shown in Table 1.

From this observation it might follow that if someone tests only the harmonic distortion in this hypothetical nonlinear suspension, he might come to a conclusion that this suspension is impaired predominantly by the third harmonic distortion and to a lesser degree by the fifth har-

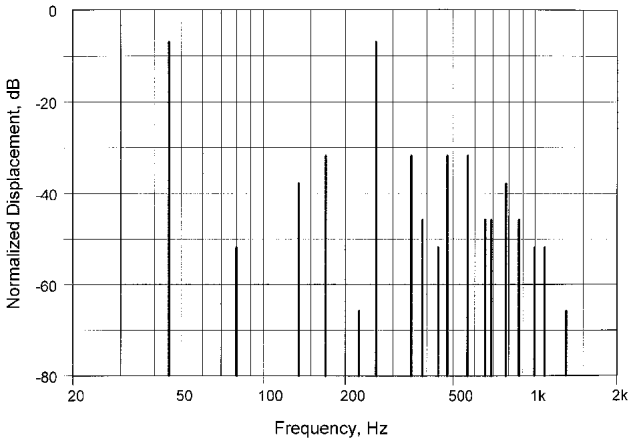

Fig. 4. Spectrum of nonlinear reaction to two-tone input; fifth-order approximation.

monic distortion. This conclusion might lead to a "picture" of a musical signal contaminated predominantly with third and slightly with fifth-order harmonic distortion. However, the application of a more complex two-tone signal changes the reaction of this nonlinear system. For example, the fifth harmonic becomes very small and virtually unessential compared to other distortion components. In its turn, the power of the stronger third harmonic becomes negligible compared to the power of the intermodulation products. This observation can be extrapolated easily to higher order static nonlinearities.

This simple example illustrates the fact that harmonics and intermodulation products are merely symptoms of nonlinearity. They are the reaction of a nonlinear system to a particular input signal. Different inputs produce different symptoms in the same nonlinear system. Since a real musical signal is a set of various spectral components rather than a merely sinusoidal tone, we can assume that the share of harmonics is much less significant than the share of intermodulation products if a musical signal is applied to a static nonlinear system. The relationship between harmonics and intermodulation products in dynamic nonlinear systems will be analyzed in detail in the next sections.

The preceding example illustrated the different reactions of the same static nonlinear system to different signals. Now let us consider the role played by the static nonlinearity of different orders. Let the hypothetical nonlinear suspension be approximated by the expression $x(t) = c_1F(t) - c_3F^3(t)$ and let the sinusoidal signal be applied to it,

$$\begin{aligned} x(t) &= c_1F \sin \omega t - c_3F^3 \sin^3 \omega t \\ &= c_1F \sin \omega t - c_3F^3(0.75 \sin \omega t - 0.25 \sin 3\omega t). \end{aligned} \quad (4)$$

Fig. 5 illustrates the dependence of displacement on the driving force and the spectrum of displacement corresponding to sinusoidal input.

A sinusoidal input obviously produces third harmonics. It also produces the spectral component of the "first order," which has the same frequency as the input signal. If a two-tone signal is applied to the same system, it produces four intermodulation products, two third harmonics, and two terms of the "first order,"

$$\begin{aligned} x(t) &= c_1F \cdot 0.5(\sin \omega_1 t + \sin \omega_2 t) \\ &\quad - c_3F^3 \cdot 0.5^3(\sin \omega_1 t + \sin \omega_2 t)^3 \\ &= c_1F \cdot 0.5(\sin \omega_1 t + \sin \omega_2 t) \\ &\quad - c_3F^3 \cdot 0.125[-0.25 \sin 3\omega_1 t - 0.25 \sin 3\omega_2 t \\ &\quad + 2.25 \sin \omega_1 t + 2.25 \sin \omega_2 t \\ &\quad - 0.75 \sin (2\omega_1 + \omega_2)t + 0.75 \sin (2\omega_1 - \omega_2)t \\ &\quad - 0.75 \sin (2\omega_2 + \omega_1)t + 0.75 \sin (2\omega_2 - \omega_1)t]. \end{aligned} \quad (5)$$

If we set the coefficient $c_3 = 0.30888$ to produce 10% THD at the single-tone input, and if we set the maximum level of the two-tone signal equal to the amplitude of a single tone, we obtain the level of harmonic components listed in Table 2.

If someone compares the measurement results of harmonic distortion produced by the two hypothetical suspensions he might come to the conclusion that they perform essentially similarly because their THD is equal to 10%, the levels of their third harmonics are close (–21.7 dB versus –22.3 dB), and the fifth harmonic produced by the fifth-order suspension is small and not important. However, the larger number of intermodulation products produced by the fifth-order nonlinearity (which remained beyond the scope of this particular harmonic measurement)

Table 1

Single Tone			Two Tones		
Harmonics			Harmonics		
1st	3rd	5th	1st	3rd	5th
–1.6 dB	–21.7 dB	–35.7 dB	–7.0 dB	–37.8 dB	–65.8 dB

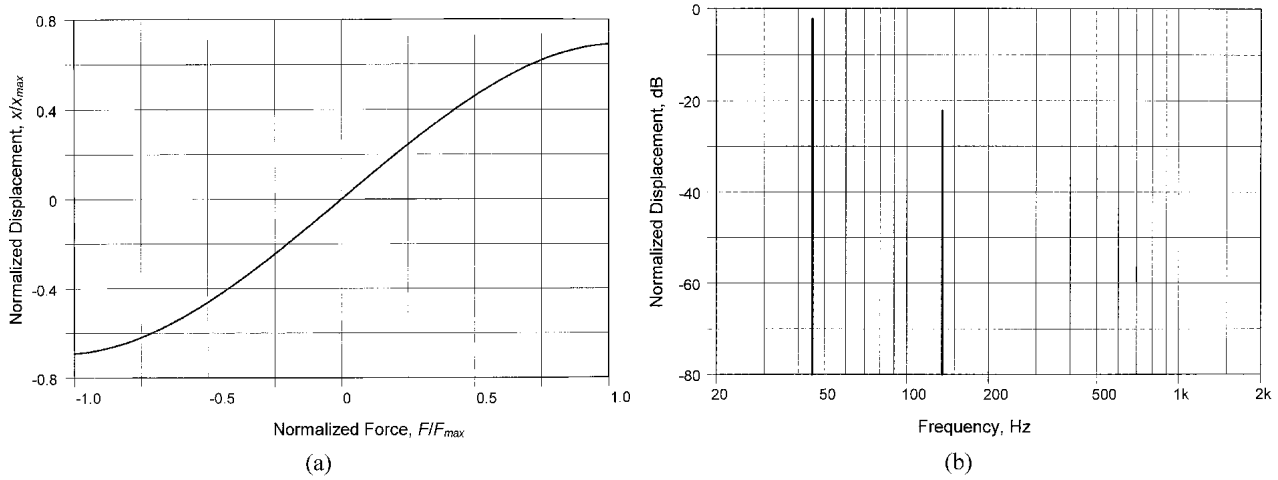

Fig. 5. (a) Dependence of suspension displacement on force; third-order approximation. (b) Spectrum of displacement corresponding to third-order approximation. Sinusoidal input.

might produce a different effect on the perceived sound quality. Fig. 6 illustrates the output spectrum. The spectrum of the distortion products is wider and the density of the spectrum is higher in the fifth-order suspension. It may cause higher perceptibility of nonlinear distortion in the fifth-order system because some distortion products might not be masked by a hearing system.

This simple example illustrates a situation when the measurement of only harmonics does not convey enough information about the performance of even a simple static nonlinear system. It also shows that a higher order static nonlinearity produces a larger number of intermodulation products if excited by a similar input signal.

Three conclusions follow.

1) The overall level of harmonics is typically lower than the overall level of intermodulation products within the same nonlinear system, and this difference is stronger in a system impaired by a higher order nonlinearity.

2) A nonlinear system of a higher order being exposed to a complex signal produces more intermodulation products with a wider spectrum. This effect is not revealed by an analysis of the harmonic distortion.

3) The wider spectrum of intermodulation products might be more noticeable because some of the spectral components would not be masked by the hearing system.

Table 3 shows the reaction of second- and third-order static nonlinearity to different multitone stimuli. The number of intermodulation products of static nonlinearity characterized by only second and third orders increases dramatically with the number of input testing tones compared to the number of harmonics. It can also be observed that the third-order nonlinearity produces the same number of harmonic products (compared to the second order) but a significantly larger amount of intermodulation products. This tendency increases in higher order nonlinearities.

In this example the increase in the number of intermodulation products generated stems from the nature of the testing signal (multitone) that was chosen for some affinity with a musical signal. Truly, the multitone stimulus is closer to a musical signal than the single-tone stimulus in the crest factor, the spectrum, and the probability density function. This example illustrates the dominance of intermodulation products revealed by the multicomponent testing signals. The tendency of intermodulation products to dominate harmonics, illustrated here through the use of a multitone signal, can be extrapolated to a musical signal. More details on this subject can be found in [1].

Table 2

Single Tone		Two Tones	
Harmonics		Harmonics	
1st	3rd	1st	3rd
−2.3 dB	−22.3 dB	−7.7 dB	−40.3 dB

3.2 THD and Harmonic Distortion

By observing only harmonic distortion curves we might not be able to come to an accurate conclusion about the entire nonlinear properties of a loudspeaker under test, and we cannot predict how the distortion products generated in a musical signal will be masked by the hearing system. In addition, harmonic distortion measurements may not reveal some nonlinear effects at all. A typical example is the Doppler distortion in direct-radiating loudspeakers. This distortion is not revealed by a single tone. At least two tones are required.

The "supremacy" of intermodulation distortion may lead to the straightforward but wrong conclusion that harmonic distortion is irrelevant in any application and may be omitted in measurements of loudspeaker nonlinear distortion. However, while not being able to characterize nonlinearity in its entirety and complexity, and link it to the audibility of signal deterioration, the harmonic distor-

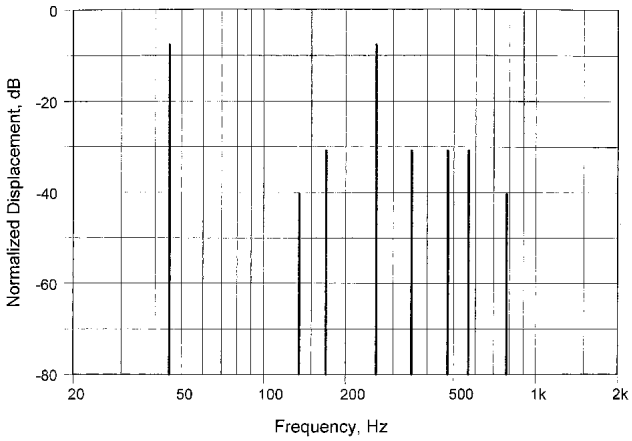

Fig. 6. Spectrum of nonlinear reaction to two-tone input; third-order approximation.

Table 3

Number of Initial Tones	Second-Order Nonlinearity		Third-Order Nonlinearity		Overall (Second and Third)	
	Number of All IM Products	Number of All Harmonics	Number of All IM Products	Number of All Harmonics	Number of All IM Products	Number of All Harmonics
1	0	1	0	1	0	2
2	2	2	4	2	6	4
3	6	3	16	3	22	6
4	12	4	40	4	52	8
5	20	5	80	5	100	10
10	90	10	660	10	750	20
15	210	15	2240	15	2450	30
20	380	20	5320	20	5700	40

tion curves, plotted separately as a function of frequency and level of input signal, provide useful information about loudspeaker under test. For example, a strong level of high-order harmonics may be indicative of a rubbing voice coil or the presence of nonlinear breakups of a compression driver's metallic diaphragm and suspension. The relationship between harmonics of even and odd orders tells about the symmetry (or the lack of it) in loudspeaker displacement-dependent parameters. The buildup of high-order harmonics with an increase in input voltage may be indicative of approaching the limit of a spider's deflection. When performing harmonic distortion measurements, one should keep in mind that the harmonics will be accompanied by an outweighing number of intermodulation products as soon as the testing tone is replaced by a musical signal.

The THD test can be used legitimately in "passed–not passed" production tests where similar types of loudspeakers are tested. Certainly, THD gives an idea about audibly noticeable nonlinear distortion if its level is high. A loudspeaker having 50% THD in the midrange will hardly be a source of mellifluous sound. It does not take some other sophisticated analysis of nonlinearity or fine listening tests to figure that out.

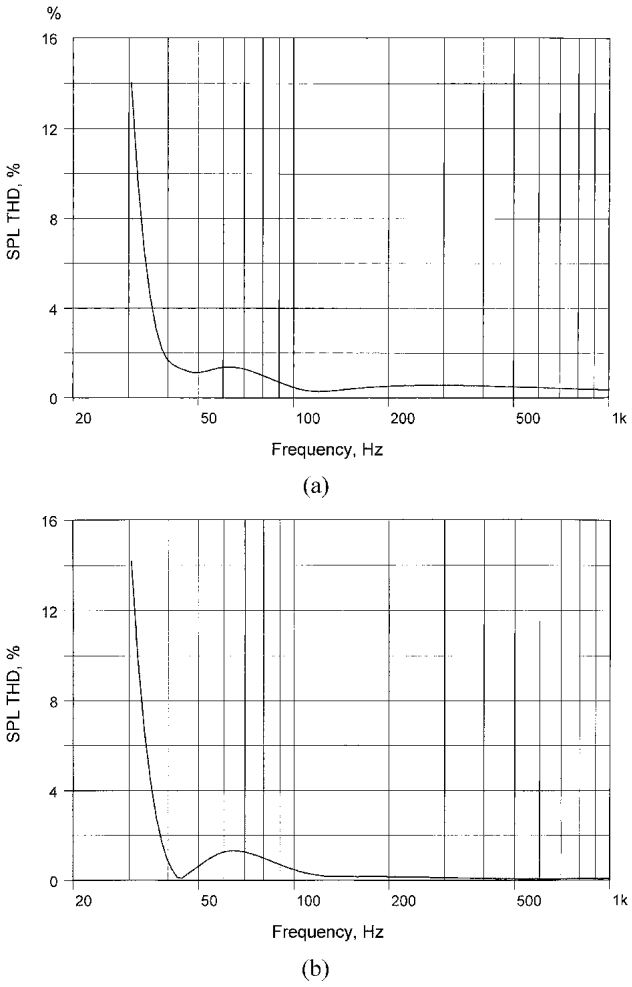

Fig. 7. SPL THD of 12-in (305-mm) woofer. Nonlinearity is produced by *Bl* product, suspension stiffness, voice-coil inductance, and flux modulation. Input voltage 10 V. (b) Same as (a), but flux modulation omitted.

Fig. 7 illustrates the sensitivity of THD test results to variations of the loudspeaker parameters. Fig. 7(a) corresponds to input voltage of 10 V applied to a nonlinear dynamic model of a 12-in (305-mm) woofer characterized by a nonlinear *Bl* product, suspension stiffness, voice-coil inductance, and flux modulation. The parameters of the woofer are given in Appendix 1. The modeling was carried out through numerical solution of a system of nonlinear differential equations describing the behavior of an electrodynamic loudspeaker (see Appendix 2). Fig. 7(b) shows the THD curve corresponding to the same woofer, but the flux modulation distortion is omitted. The difference in the physical properties between the two models is reflected in the difference in THD curves. It can be observed that the flux modulation distortion affects the THD curve at high frequencies. It is convenient to overlay THD curves corresponding to different input levels. Fig. 8 shows SPL THD curves corresponding to an increase of the input voltage from 10 to 40 V in 3-dB increments.

Figs. 9 and 10 show THD curves corresponding to two 8-in (203-mm) woofers having different motors. (One has a long 12-mm coil and a 6-mm short gap, the other a short 6-mm coil and a long 12-mm gap.) The parameters of the woofers are given in Appendix 1. The level of the input signals corresponds to maximum voice-coil displacements of 4 and 10 mm. The difference in the THD curves of the small-level signal a is pronounced at low frequencies, whereas the difference in the large-level signal b is pronounced at frequencies above 80 Hz. Therefore THD gives an idea of the difference in the objective performance of two loudspeakers being compared.

3.3 High-Order Frequency Response Functions (Frequency-Domain Volterra Kernels)

All the foregoing conclusions concerning the deficiency of information about loudspeaker nonlinearity provided by harmonic and THD measurements do not mean, however, that a frequency response of traditionally measured individual intermodulation products of the second or third orders will always represent accurately the nonlinear properties of a loudspeaker in their entire complexity. The following example will illustrate a situation when neither

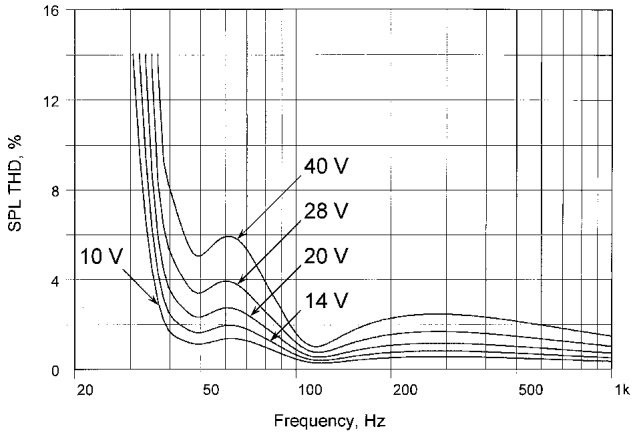

Fig. 8. Increase in SPL THD of 12-in (305-mm) woofer corresponding to increase in input voltage from 10 to 40 V in 3-dB increments.

the second harmonic nor the second-order difference-frequency intermodulation products provides sufficient information about the distortion of a hypothetical loudspeaker characterized by only a second-order nonlinearity. Figs. 11 and 12 show second-order frequency responses (frequency-domain Volterra kernels of the second order) of the same 8-in (203-mm) woofers having different motors. A typical HFRF is presented in the form of a three-dimensional "mountain terrain" with two horizontal frequency axes. Figs. 11(a) and 12(a) illustrate the three-dimensional terrains of the second distortion products, whereas Figs. 11(b) and 12(b) show the maps of this surface. The vertical axis shows the level of *all* second-order distortion frequency responses, including second harmonics, the sum and difference intermodulation products at *all* combinations of two frequencies, and the frequency-dependent constant component (dc or zero harmonic) if it is excited in a particular nonlinear system [see Figs. 11(a) and 12(a)].

In this interpretation the Cartesian coordinates of a point on this map corresponding to one negative and one positive frequency describe the second-order *difference* frequency component $P_{f_2-f_1}$, whereas a point with the coordinates belonging to both positive frequencies is a second-order *sum* intermodulation product $P_{f_2+f_1}$. The diagonal line a, characterized by the equal in modulus but opposite in sign frequencies, describes the zero-order harmonic $P_{f_1-f_1}$, which is a constant displacement if the HFRF describes the voice-coil excursion. The diagonal line characterized

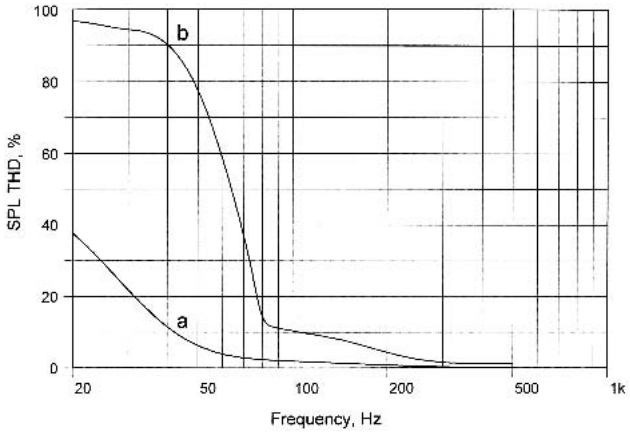

Fig. 9. SPL THD corresponding to voice-coil maximum displacement. Loudspeaker A (long coil, short gap). a—X_{max} = 4 mm; b—X_{max} = 10 mm.

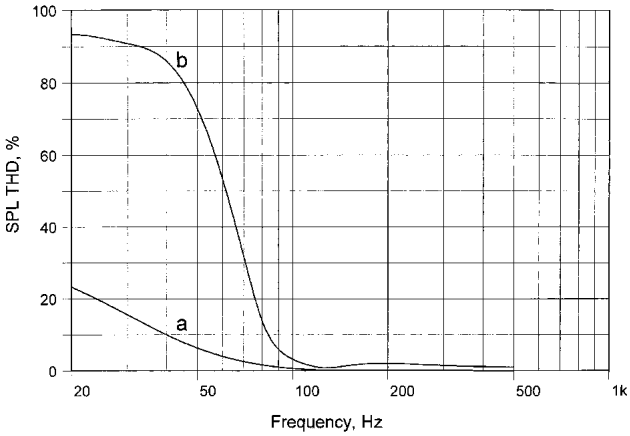

Fig. 10. SPL THD corresponding to voice-coil maximum displacement. Loudspeaker B (short coil, short gap). a—X_{max} = 4 mm; b—X_{max} = 10 mm.

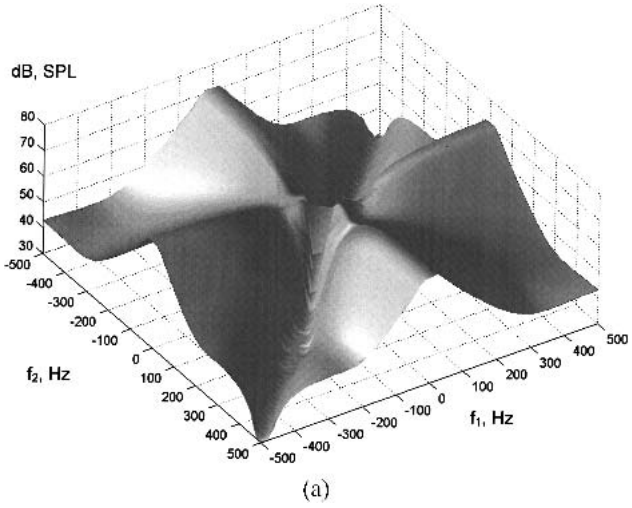

(a)

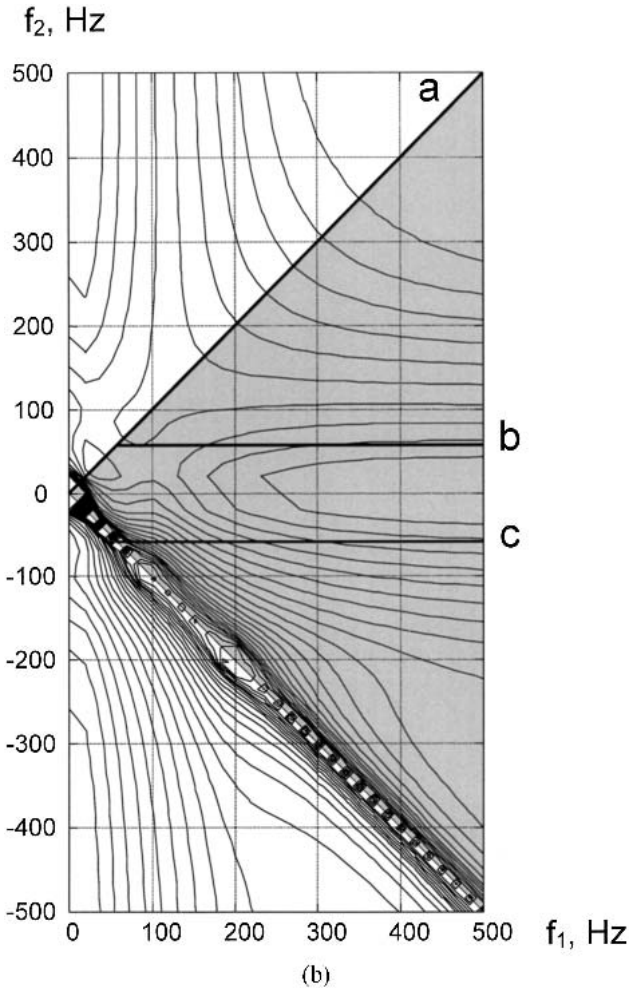

(b)

Fig. 11. Sound pressure response of loudspeaker A (long coil, short gap). (a) Second-order frequency-domain Volterra kernel. Peak level of input signal corresponds to X_{max} = 4 mm. (b) Topological view of second-order SPL response. a—second harmonic P_{2f}; b—sum intermodulation product $P_{f_2+f_1}$; c—difference intermodulation product $P_{f_2-f_1}$. Unique area of kernel is highlighted.

by the equal values of positive frequencies is a second harmonic distortion $P_{f_1+f_1}$ (see Figs. 11 and 12). By comparing the second harmonic distortion cut with the entire surface of the second-order distortion, one may clearly see what a small share of all the information required to describe entire second-order nonlinearity is represented by the single second harmonic distortion response. To know the dynamic reaction of the second-order nonlinearity we should also take into account the three-dimensional surface of the second-order phase response and perform a twofold inverse Fourier transform, which will obtain the second-order impulse response. Two-dimensional convolution of the input signal with this two-dimensional pulse response provides the dynamic reaction of the second-order nonlinearity. It is not hard to imagine how far the distortion signal may be from the results of harmonic or THD measurement. Whether or not this dynamic distortion signal is noticed by the hearing system depends on a number of factors that should be considered in the context of masking such as the level of the signal, its dynamics, and the spectral contents.

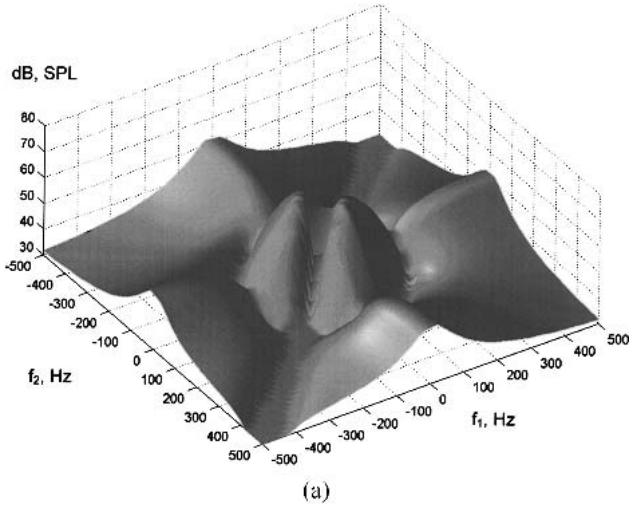

(a)

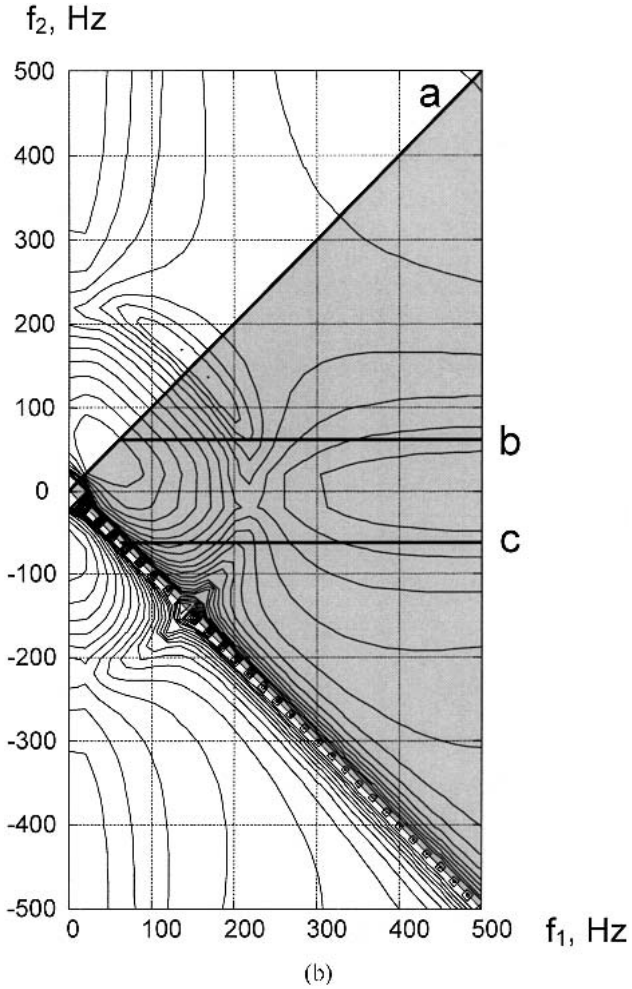

(b)

Fig. 12. Sound pressure response of loudspeaker B (short coil, long gap). (a) Second-order frequency-domain Volterra kernel. Peak level of input signal corresponds to $X_{\max} = 4$ mm. (b) Topological view of second-order SPL response. a—second harmonic P_{2f}; b—sum intermodulation product $P_{f_2+f_1}$; c—difference intermodulation product $P_{f_2-f_1}$. Unique area of kernel is highlighted.

The concept of Volterra expansion can be formally extended to higher orders. Unfortunately the third-order nonlinearity needs four-dimensional space for its description (three frequency scales), which defies simple graphic representation. One possible solution to plot the third-order HFRFs is a cut through one of the three frequency scales corresponding to the worst case of distortion, and using the remaining two scales in the three-dimensional graph. Reed and Hawksford used this approach in [17]. For the higher orders of nonlinearity the situation becomes even more desperate, and graphical representation is even less practical. To make matters worse, with increasing orders of nonlinearity the volume of calculations required to describe a Volterra model increases tremendously, making a practical application impossible. This "curse of dimensionality" is clearly illustrated by an analysis of the expression for the output signal of a nonlinear system described by the first three terms of a Volterra expansion,

$$y(t) = \int_0^t h_1(\tau_1)x(t-\tau)\,d\tau + \int_0^t\int_0^t h_2(\tau_1,\tau_2)x(t-\tau_1) \times x(t-\tau_2)\,d\tau_1\,d\tau_2 + \int_0^t\int_0^t\int_0^t h_3(\tau_1,\tau_2,\tau_3)x(t-\tau_1) \times x(t-\tau_2)x(t-\tau_3)\,d\tau_1\,d\tau_2\,d\tau_3. \quad (6)$$

Here $h_2(\tau_1, \tau_2)$ is a second-order kernel, or a two-dimensional impulse response, which depends on the two time arguments τ_1 and τ_2. Correspondingly, $h_3(\tau_1, \tau_2, \tau_3)$ is a third-order kernel, depending on three time arguments.

If, for example, the analysis of the first-order kernel (linear impulse response) is carried out on one thousand samples, the second-order kernel (second-order impulse response) requires one-quarter million samples to be analyzed with analogous resolution. The analysis of the third-order kernel with the same resolution amounts to 375 million samples, whereas the fourth-order kernel requires 250 billion samples to keep the same accuracy. In this estimation the property of Volterra kernel symmetry was used and the redundant parts of kernels were omitted.

Unique areas of the second-order kernels presented are highlighted in Figs. 11(b) and 12(b). One quarter of all possible permutations of the samples of the second-order system is required to describe the system. Three-eighths of

all possible permutations of the third-order system's response samples is enough to describe it completely, and one-fourth of all permutations of the fourth-order samples [14]. Still, the number of samples to be analyzed increases enormously with an increase in the order of Volterra expansion.

The calculation of HFRFs from multidimensional pulse responses needs n-fold Fourier transforms. The volume of calculations also increases significantly with an increase in the order of nonlinearity,

$$\begin{aligned}
H_1(\mathrm{i}\omega_1) &= \int_{-\infty}^{\infty} h_1(\tau_1)\mathrm{e}^{-\mathrm{i}(\omega_1\tau_1)}\,\mathrm{d}\tau_1 \\
H_2(\mathrm{i}\omega_1, \mathrm{i}\omega_2) &= \int_{-\infty}^{\infty} h_2(\tau_1, \tau_2)\mathrm{e}^{-\mathrm{i}(\omega_1\tau_1+\omega_2\tau_2)}\,\mathrm{d}\tau_1\,\mathrm{d}\tau_2 \\
H_3(\mathrm{i}\omega_1, \mathrm{i}\omega_2, \mathrm{i}\omega_3) &= \int_{-\infty}^{\infty} h_3(\tau_1, \tau_2, \tau_3)\mathrm{e}^{-\mathrm{i}(\omega_1\tau_1+\omega_2\tau_2+\omega_3\tau_3)} \\
&\quad \mathrm{d}\tau_1\,\mathrm{d}\tau_2\,\mathrm{d}\tau_3 \\
&\quad \vdots \\
H_n(\mathrm{i}\omega_1, \ldots, \mathrm{i}\omega_n) &= \int_{-\infty}^{\infty} h_n(\tau_1, \ldots, \tau_n)\mathrm{e}^{-\mathrm{i}(\omega_1\tau_1+\cdots+\omega_n\tau_n)} \\
&\quad \mathrm{d}\tau_1 \ldots \mathrm{d}\tau_n.
\end{aligned} \tag{7}$$

In addition, the Volterra series expansion has a fundamental constraint stemming from the assumption that there is no energy exchange between nonlinear products of different orders. This constraint confines the application of Volterra series expansions to only weakly nonlinear systems. Attempting to use Volterra expansions for a nonlinear system with a strong nonlinearity causes divergence of the Volterra series.

This simple example illustrates why Volterra expansions of orders higher than three are practically never used. It precludes Volterra expansion from handling strong and high-order nonlinearities. The measurement of Volterra HFRFs can be carried out using special signals, such as maximum-length sequences (MLS) [27], multitone stimuli [28], and Gaussian noise [29]. There are methods providing a direct calculation of HFRFs from NARMAX output data [30]. Straightforward methods operating with a variation of two or three sinusoidal signals are not practical because of the measurement time burden.

3.4 Two-Tone Intermodulation Frequency Responses

Measuring the frequency responses of intermodulation products by using a two-tone signal has nearly as old a history as measuring harmonic distortion and THD. Two methods have been used predominantly in the audio industry. One, proposed by Hilliard, uses one fixed low-frequency tone and one sweeping tone. The method was adopted by SMPTE [19]. It is often called the modulation method. The second method, using two sweeping tones and keeping the frequency difference between them constant, was proposed by Scott [20]. It is called difference frequency or CCIF method. If a two-tone signal is applied to a second-order nonlinear system, it generates the following distortion products: dc component, two different intermodulation spectral components (sum and difference products), and two second harmonics. Meanwhile the nonlinear reaction of the third-order nonlinearity to the same two-tone signal will consist of two third-order harmonics, two spectral components having the same frequencies as the initial tones but lower amplitudes, and four intermodulation products. However, it is known from the theory of nonlinear systems that full description of the third-order nonlinearity formally needs at least a three-tone signal [14]. This increases the number of third-order harmonics to three, and the number of spectral components having input signal frequencies to three as well. The number of intermodulation products goes as high as 16.

It is not practical to plot 16 different frequency responses of intermodulation products. Traditionally only the products $P_{f_2\pm 2f_1}$ are analyzed, omitting components of the type $P_{f_3\pm f_2\pm f_1}$, which are also generated by the third-order nonlinearity. Hence the measurement of individual intermodulation products of the second and third orders gives limited information about the third-order nonlinearity if a two-tone signal is used. With regard to higher order nonlinearity, the standardized two-tone intermodulation methods supply limited information as well.

Plotting all four "conventional" intermodulation curves ($P_{f_2\pm f_1}$ and $P_{f_2\pm 2f_1}$) on a single graph still produces a picture that is difficult to comprehend and interpret. An integrated criterion in the form of total intermodulation distortion (TIMD) is a simplifying solution, leading to fewer frequency responses of intermodulation distortion. For example, standard IEC 60268-5 [22] determines: "The modulation distortion (MD) of the nth order shall be specified as the ratio of the arithmetic sum of the r.m.s. values of the sound pressures due to distortion components at frequencies $f_2 \pm (n-1)f_1$ to the r.m.s. value of the sound pressure P_{f_2} due to the signal f_2." The total intermodulation coefficient of the second order according to IEC 60268-5 is

$$d_2 = \frac{P_{f_2-f_1} + P_{f_2+f_1}}{P_{f_2}} \times 100\%. \tag{8}$$

The total intermodulation coefficient of the third order is

$$d_3 = \frac{P_{f_2-2f_1} + P_{f_2+2f_1}}{P_{f_2}} \times 100\%. \tag{9}$$

The frequencies f_1 and f_2 satisfy the condition $f_2 >> f_1$, and the ratio of the amplitudes of the input signal is specified by the user. The standard gives no recommendation regarding the measurement of intermodulation and harmonic products having orders higher than three. This omission was probably due to practical concerns. Without calling into question the validity of the standard's recommendations, the authors do not exclude situations when measuring higher order harmonic and intermodulation products might be useful in the assessment of audio equipment performance.

As was mentioned in Section 2, higher order nonlinear products may be more detrimental to the sound quality compared to the lower order products. This effect was recognized a long time ago (see, for example, [31]), and modern research confirms it [1], [32]. The importance of higher order distortion products is somewhat twofold. First, high-order nonlinearity produces a very large number of intermodulation products, whose number and energy increase dramatically with an increasing input signal level. Second, higher order products are usually spread over a wide frequency range, which results in weaker psychoacoustic masking of these distortion products [1]. In the wake of it, the authors developed an alternative way to formulate two-tone intermodulation distortion characteristics. Figs. 13 and 14 show the two-tone intermodulation distortion curves of the same two 8-in (203-mm) woofers. The distortion curves correspond to similar 10-mm maximum voice-coil displacement. The difference between these intermodulation distortion curves of the two loudspeakers is significantly more pronounced when compared with the THD curves of the same woofers. The intermodulation distortion curves presented in Figs. 13 and 14 are calculated differently from traditional intermodulation coefficients recommended by existing standards. The two-tone intermodulation distortion (TIMD) is specified by the authors as

$$d_{\mathrm{TIMD}}(f) = \frac{\sqrt{\sum_{i=1}^{N} p_i^2(f)}}{P_f} \times 100\% \tag{10}$$

where

$$p_1(f) = P_{f_2+f_1}, \quad p_2(f) = P_{f_2-f_1}, \quad p_3(f) = P_{f_2+2f_1},$$
$$p_4(f) = P_{f_2-2f_1}, \quad p_5(f) = P_{f_2+3f_1}, \quad p_6(f) = P_{f_2-3f_1},$$
$$p_7(f) = P_{f_2+4f_1}, \quad p_8(f) = P_{f_2-4f_1}, \ldots$$
$$p_{n-1}(f) = P_{f_2+mf_1}, \quad p_n = P_{f_2-mf_1}$$

are the amplitudes of the intermodulation products, $P_f = P_{f_1} = P_{f_2}$ is the amplitude of either one of the fundamental tones, f_1 is the fixed low-frequency tone, and f_2 is the higher frequency sweeping tone.

In this approach the excitation signal consists of two tones having equal amplitude. One of these two tones is swept across the frequency range. The level of distortion, calculated according to Eq. (10), is plotted at the frequency of the sweeping tone. The authors attempted to extend the recommendations of IEC 60268-5 [22] to the

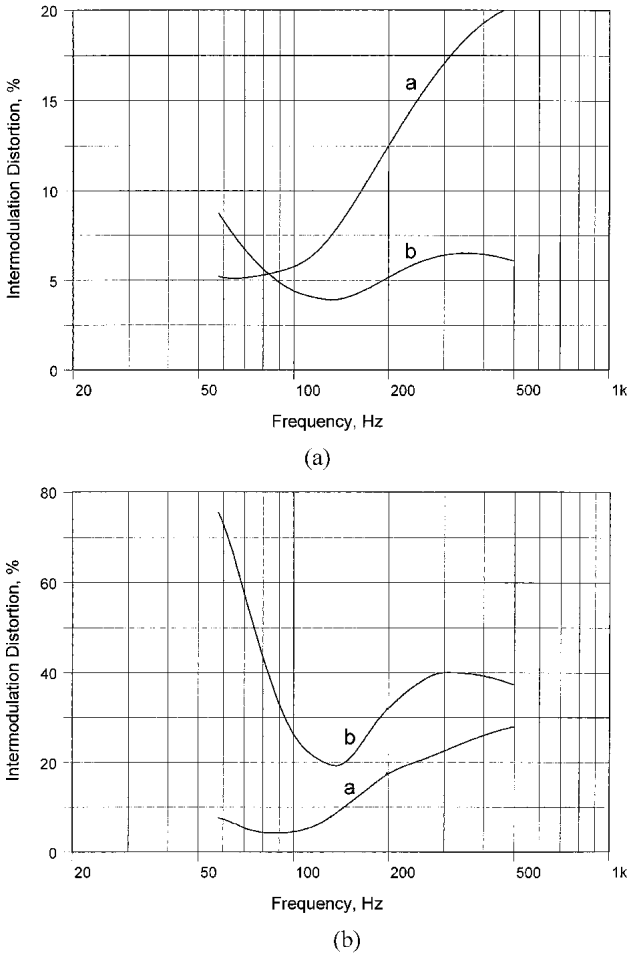

Fig. 13. Two-tone intermodulation distortion (IEC 60268-5); loudspeaker A (long coil, short gap). a—$(P_{f_2-f_1} + P_{f_2+f_1})/P_{f_1}$; b—$(P_{f_2-2f_1} + P_{f_2+2f_1})/P_{f_1}$. (a) Voice-coil maximum displacement $X_{\max} = 4$ mm. (b) Voice-coil maximum displacement $X_{\max} = 10$ mm.

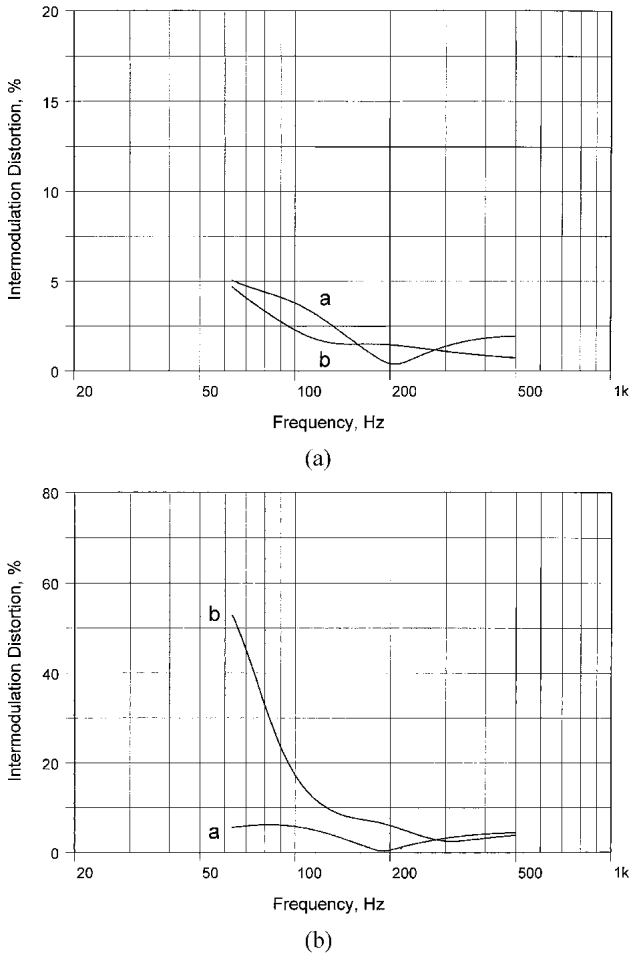

Fig. 14. Two-tone intermodulation distortion (IEC 60268-5); loudspeaker B (short coil, long gap). a—$(P_{f_2-f_1} + P_{f_2+f_1})/P_{f_1}$; b—$(P_{f_2-2f_1} + P_{f_2+2f_1})/P_{f_1}$. (a) Voice-coil maximum displacement $X_{\max} = 4$ mm. (b) Voice-coil maximum displacement $X_{\max} = 10$ mm.

measurement of two-tone intermodulation distortion in the form of the intermodulation products having frequencies ($f_2 \pm f_1$) and ($f_2 \pm 2f_1$). The latter are the products of the interaction between the first and second harmonics; the first tone with the first harmonic of the second tone. The authors merely extended the set of harmonics of the first signal to higher orders ($3f_1$, $4f_1$), which led to intermodulation terms of the kind ($f_2 \pm 3f_1$), ($f_2 \pm 4f_1$). The intermodulation terms corresponding to the interaction between the harmonics of the first tone and the harmonics of the second tone, such as ($2f_2 \pm 2f_1$), ($3f_2 \pm 2f_1$), ($2f_2 \pm 3f_1$), ($3f_2 \pm 3f_1$), etc., were omitted. The authors do not claim the ultimate validity of this approach. Including all the intermodulation products produced by two-tone excitation would probably provide more accurate results.

An alternative method to measure intermodulation distortion has been used by Keele [23], [24]. His test signal, consisting of two tones, 40 Hz and 400 Hz, of equal amplitude, is applied to a loudspeaker, the input level is increased, and the intermodulation is measured and plotted as a function of the input level. Such a test is a simple way to evaluate the intermodulation of the midrange output of a loudspeaker by a simultaneous bass signal.

In the current work Keele's general approach to measuring intermodulation distortion versus input level was simulated using two different criteria. The first, d_{TTIMD}, includes all N measurable output intermodulation products; the second, d_{TTHD}, takes into account only M harmonic distortion products produced by two primary tones. Here TTIMD stands for two-tone total intermodulation distortion and TTHD designates two-tone total harmonic distortion

$$d_{\mathrm{TTIMD}} = \frac{\sqrt{\sum_{i=1}^{N} P(i)_{\mathrm{IM}}^2}}{P_f} \times 100\% \tag{11}$$

$$d_{\mathrm{TTHD}} = \frac{\sqrt{\sum_{k=1}^{M} P(k)_{\mathrm{H}}^2}}{P_f} \times 100\% \tag{12}$$

where $P(i)_{IM}$ is the amplitude of an intermodulation product corresponding to the ith frequency, $P(k)_{\mathrm{H}}$ is the amplitude of the harmonic corresponding to the kth frequency, and N and M are the number of intermodulation and harmonic products, respectively. To avoid the overlapping of the fundamentals and the distortion products, the frequencies of the primary tones were chosen as $f_1 = f_s$ and $f_2 = 5.5f_s$ with frequency f_s being the resonance frequency of the loudspeaker.

Figure 15 shows the graphs of two-tone total intermodulation and harmonic distortion of two 8-in (203-mm) woofers as a function of the input level. The frequencies of the tones are 57 and 313.5 Hz. The harmonic distortion of the loudspeaker with the long voice coil a prevails at the lower level of the input signal. However, this effect is not observed when the two-tone signal is replaced by a ten-tone input signal (Fig. 16). Here the concept of two-tone total harmonic and intermodulation distortion is extended to a larger number of input tones. The ten-tone total harmonic distortion coefficient takes into account the harmonics of all input tones. The level of this distortion, similar to the TTIMD, is related to one of the fundamental tones. This simplifies the comparison of the distortions evaluated by these two criteria.

3.5 Multitone Stimulus

The possible circumvention of the partial "blindness" of the conventional two-tone intermodulation tests is not to plot continuous frequency responses of the corresponding intermodulation products, but rather to show the full discrete spectra of all nonlinear products corresponding to particular frequencies and levels of the two test tones. By extending this idea to a larger number of excitation tones, we naturally arrive at the concept of the multitone signal. Indeed, if we obtain and graph the spectrum of a nonlinear reaction to the two-tone signal, which, as it has been shown, gives limited information even about the third-order nonlinearity, let alone the higher orders, why not use as many tones as it takes to detect all conceivable higher

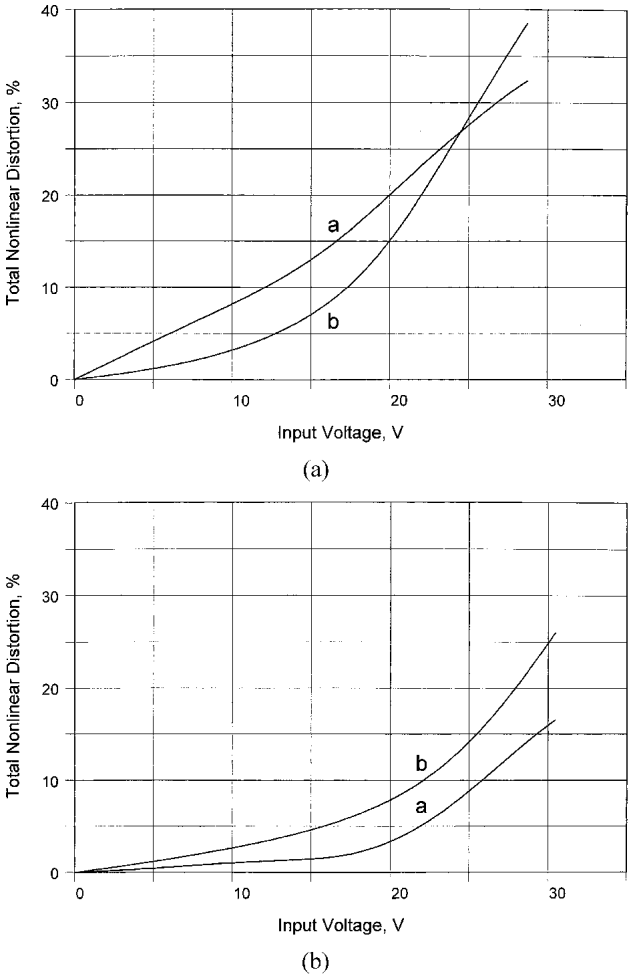

Fig. 15. Two-tone total nonlinear distortion as a function of input voltage. a—intermodulation products; b—harmonic products. (a) Loudspeaker A (long coil, short gap.). $f_1 = f_s = 57$ Hz; $f_2 = 5.5 \cdot f_1 = 313.5$ Hz. $U_{\max} = 29$ V corresponds to $X_{\max} = 10$ mm. (b) Loudspeaker B (short coil, long gap). $f_1 = f_s = 62$ Hz; $f_2 = 5.5 \cdot f_1 = 341$ Hz. $U_{\max} = 31$ V corresponds to $X_{\max} = 10$ mm.

order intermodulation products, cover the entire frequency range of measurement, and have a signal statistically much closer to the real musical signal than a single-tone or two-tone signal?

This idea can be extended to a tone in every FFT frequency bin. This abundance of tones turns the multitone stimulus into a noiselike signal. Truly, noise signals are used widely in the identification and analysis of nonlinear systems as, for example, in the measurement of the coherence function. However, once the FFT is applied to the output signal of a nonlinear system excited by such noiselike signals, all individual distortion spectral components are obscured by the fundamental tones and become invisible on a graph. Meanwhile the multitone signal, producing a "sparse" and discrete spectrum at the output of a nonlinear system, makes the majority of distortion products visible on a graph. At the same time the multitone signal is rather close to noise and musical signals in the probability density function, bandwidth, and crest factor. The multitone stimulus fills the gap between the noise-based methods of nonlinear identification and measurements, and the traditional standardized methods using one or two stationary or swept (stepped) tones.

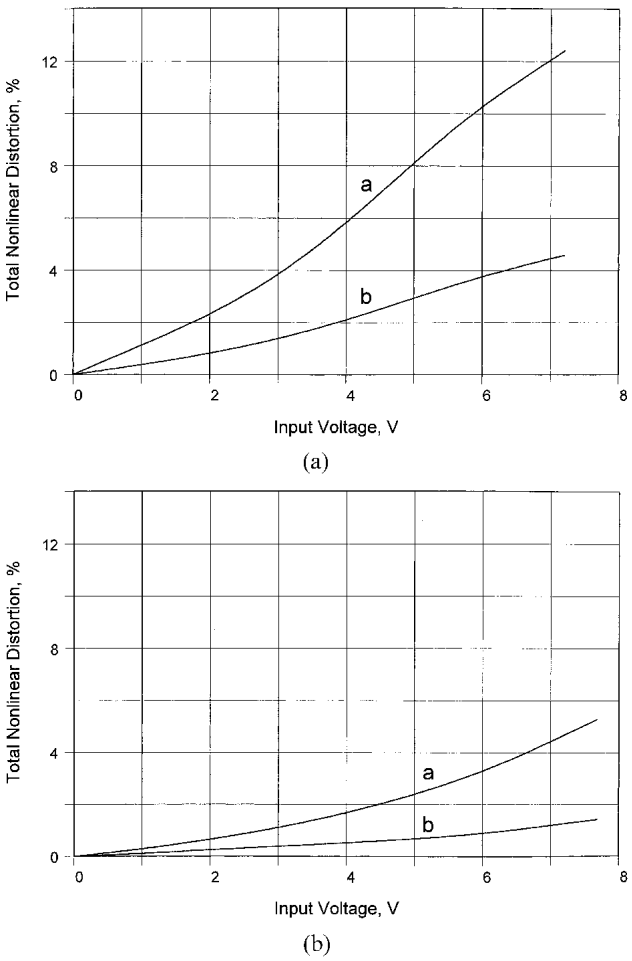

Fig. 16. Ten-tone total nonlinear distortion as a function of input voltage. a—intermodulation products; b—harmonic products. Logarithmic frequency distribution in frequency range f_s to $5.5 f_s$. (a) Loudspeaker A (long coil, short gap). $U_{max} = 7.3$ V corresponds to $X_{max} = 10$ mm. (b) Loudspeaker B (short coil, long gap). $U_{max} = 7.8$ V corresponds to $X_{max} = 10$ mm.

Usually the multitone signal is generated according to the simple rule

$$x(t) = \sum_{i=1}^{N} A_i \sin(\omega_i t + \varphi_i). \tag{13}$$

A strong advantage of the multitone stimulus is a short measurement time and the ability to reveal simultaneously a set of visible harmonic and intermodulation products. In this capacity the multitone signal is beyond competition with other signals. Multitone testing handles high-order nonlinearity, and its use is not hampered by the existence of such effects as hard limiting, hysteresis, and dead zone.

Also, the multitone stimulus can be used in applications where the loudspeaker short-term performance must be evaluated, such as the maximum SPL. Comparing a multitone burst with a tone burst, the advantages of the former become obvious. After the time-domain reaction of the loudspeaker to the tone burst of a particular frequency has been received and preprocessed to skip the transients and then put through the Fourier transform, only harmonic distortion and THD become available. The distortion (harmonic or THD) corresponds to only a single excitation frequency. To cover the whole frequency range of interest, these measurements have to be repeated at different frequencies. Taking into account the number of measurements needed to cover the entire frequency range with a decent resolution, the overall measurement time may be significant. Meanwhile, by applying the multitone burst, only one measurement is needed and, in addition, the multitone signal obtains more information about the nonlinearity in a loudspeaker under test. Furthermore, a multitone burst's crest factor can be "tuned" by adjusting the phases of individual spectral components.

However, the interpretation of a nonlinear reaction to a multitone stimulus may be arduous if the number of generated nonlinear products of different orders is substantial. A multitone stimulus gives such "abundant" spectral information about nonlinearities that it is difficult to comprehend at first sight. (Truly, a second look at the reaction to the multitone stimulus may not be helpful either when one has to analyze hundreds if not thousands of distortion spectral components.) In addition, an engineer has no information on how a particular pattern of nonlinear reactions to multitone stimuli is related to the perceived sound quality. Moreover, the spectrum of reactions to multitone stimuli is not convenient to overlay and compare, especially if the responses to several input levels are to be observed. There are several possible ways to overcome this impediment. One is to distinguish the products of different orders by postprocessing and to plot them either separately or in different colors on the same graph. Another solution is to plot the averaged value of all distortions located between two adjacent tones, as it is done in [10] and in the FASTTEST multitone measurement [8]. This approach permits a simple graphical representation of nonlinear distortions at different levels of input signal.

Distinguishing different intermodulation and harmonic products of different orders is comparatively easy when the number of initial tones is reasonably low (less than ten,

for example). With an increasing number of input tones overlapping of different frequencies occurs, and the problem of separation becomes much more difficult, but not a theoretically impossible task. The separation can be carried out by a discrete progressive increase of the input level accompanied by an analysis of the rate of increase of each distortion product in a particular frequency bin in such a way that the evaluated spectral components (including possible overlapped ones) measured at different levels of input signal form a so-called polynomial Vandermonde matrix [33]. Corresponding mathematical manipulations with this matrix, which remain beyond the scope of this work, provide a separation of the overlapped spectral components and make it possible to evaluate the level and phase of each, disregarding the fact that they overlap. This approach is described, for example, in [28], where a multitone signal is used in the identification of weakly nonlinear systems and the measurement of Volterra kernels.

An alternative method to represent the results of multitone testing is the averaging of distortion products in a "sliding window." The spectral components are averaged in a window (such an rectangular or Hanning), and the averaged value of the distortion products is plotted at the frequency corresponding to the center of the window [34]. Afterward the window is shifted one frequency bin "up" and the process is repeated. Ultimately it provides a continuous frequency response of the distortion products, which encapsulates all harmonics and a variety of intermodulation products generated by a particular loudspeaker at a particular level of multitone stimuli, and a particular distribution of primary tones. It has been dubbed the multitone total nonlinear distortion (MTND). One of the possible ways to calculate MTND, where the Hanning window is used, is presented in the expression

$$d_{\mathrm{MTND}}(f_i) = 20\log\left(\sqrt{\sum_{k=i-K/2}^{K/2}\left\{D_k\left[\cos\left(\frac{\pi|f_i - f_k|}{\Delta f}\right)+1\right]\frac{1}{2}\right\}^2}\Big/ p_0\right) \quad \text{(dB SPL)} \quad (14)$$

where Δf is the width of the frequency window, f_i is the window center frequency, D_k is the amplitude of a sound pressure distortion product (Pa) at the frequency f_k, and K is the number of spectral components; $p_0 = 2 \times 10^{-5}$ Pa.

The frequency window consists of K frequency bins. The window is essentially a weighting function that has a maximum at the frequency f_i corresponding to the center of the window. This way of formulating multitone distortion was chosen experimentally. The resulting frequency-dependent function $d_{\mathrm{MTND}}f)$ looks like an envelope of the distortion products.

There are other possible ways to express multitone total nonlinear distortion. For example, $d_{\mathrm{MTND}}(f)$ can be expressed as

$$d_{\mathrm{MTND}}(f_1) = 20\log\left(\sqrt{\frac{1}{K}\sum_{k=i-K/2}^{K/2} D_k^2}\Big/ p_0\right) \quad \text{(dB SPL)}. \quad (15)$$

This expression for the MTND characteristic uses a rectangular window and the weighting coefficient $1/K$, where K is the number of distortion products in the rectangular window. This way to formulate $d_{\mathrm{MTND}}(f)$ gives values that are too low if the number of distortion products in a current window is significant but the level of them is not high. This statement is purely empirical and bears no relationship to subjective sensations. An alternative way might be to omit the weighting coefficient $1/K$ entirely. In this case, however, the level of $d_{\mathrm{MTND}}(f)$ may become disproportionally high if the number of distortion products corresponding to a particular position of the rectangular window is high, even if their amplitude is low. These practical considerations mean that when the level of an MTND curve is much lower or much higher than the level of distortion spectral components, the graph of distortion looks unnatural. This is merely the authors' subjective point of view derived from numerous modeling and measurement experiments.

Fig. 17 shows the spectrum of the SPL reaction to the input multitone stimulus of the same two 8-in (203-mm) woofers. The solid curves correspond to MTND calculated according to Eq. (15). Fig. 18 shows the reaction to multitone stimuli of the 12-in (305-mm) woofer with and without flux modulation distortion. The

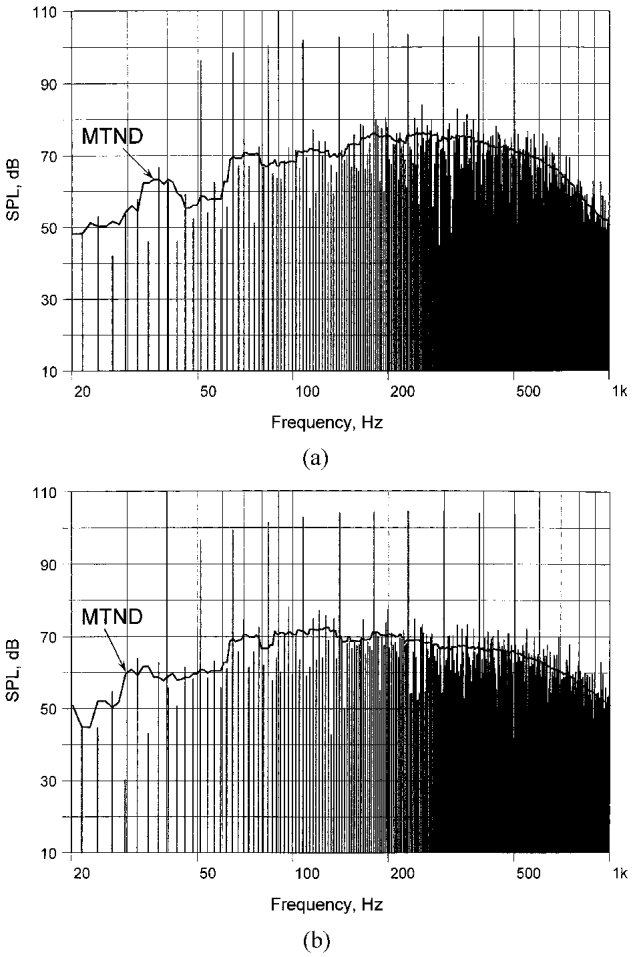

Fig. 17. Sound pressure reaction to multitone stimulus. Peak level of input signal corresponds to $X_{\max} = 10$ mm. (a) Loudspeaker A (long coil, short gap). (b) Loudspeaker B (short coil, long gap).

solid curves correspond to MTND calculated according to Eq. (14).

The presentation of the reaction of a device impaired by nonlinearity to multitone stimuli in the form of an averaged curve (MTND) makes it easy to overlay different curves belonging, for example, to different levels of input signals or to different loudspeakers. Fig. 19 shows two overlaid MTND curves, indicating that the flux modulation produces distortion in the upper part of the frequency range.

The frequency response of the MTND curve can be expressed in dB SPL [Eqs. (14) and (15)] as well as in the percentage of the fundamental frequency response,

$$d_{\mathrm{MTND}}(f_i) = \left(\sqrt{\sum_{k=i-K/2}^{K/2} \left\{ D_k \left[\cos\left(\frac{\pi |f_i - f_k|}{\Delta f} \right) + 1 \right] \frac{1}{2} \right\}^2} \Big/ A(f_i) \right) \times 100(\%) \quad (16)$$

where $A(f_i)$ is the amplitude of the frequency response of a loudspeaker at the frequency f_i.

Fig. 20 shows MTND responses of the 12-in (305-mm) woofer calculated according to Eq. (16) and at different levels of the input signal in 3-dB increments.

There is a current impediment to the widespread use of multitone stimuli for measuring nonlinearity in loudspeakers. This is the ambiguity of the nonlinear reaction of a particular device to a multitone signal. A different distribution and a different number of tones produce different reactions. In theory all these responses belong to the same multidimensional space of nonlinear reactions; however, for an observer these responses look different. This complicates the comparison of responses measured using different distributions and number of tones. So the current disadvantage of using multitone stimuli is the lack of a common agreement regarding the number of tones, their distribution, and the initial phases. To avoid this problem the number and distribution of tones should be standardized.

There are many methods of forming the frequency distribution of multitone fundamentals. The major goal of some of the frequency distributions of primary tones (different from the evenly distributed tones on a logarithmic frequency scale) is to minimize the overlapping of primary tones and distortion components [7], [12].

As was mentioned, the separation becomes increasingly difficult with an increasing order of the distortion products due to the effect of overlapping. The separation can be

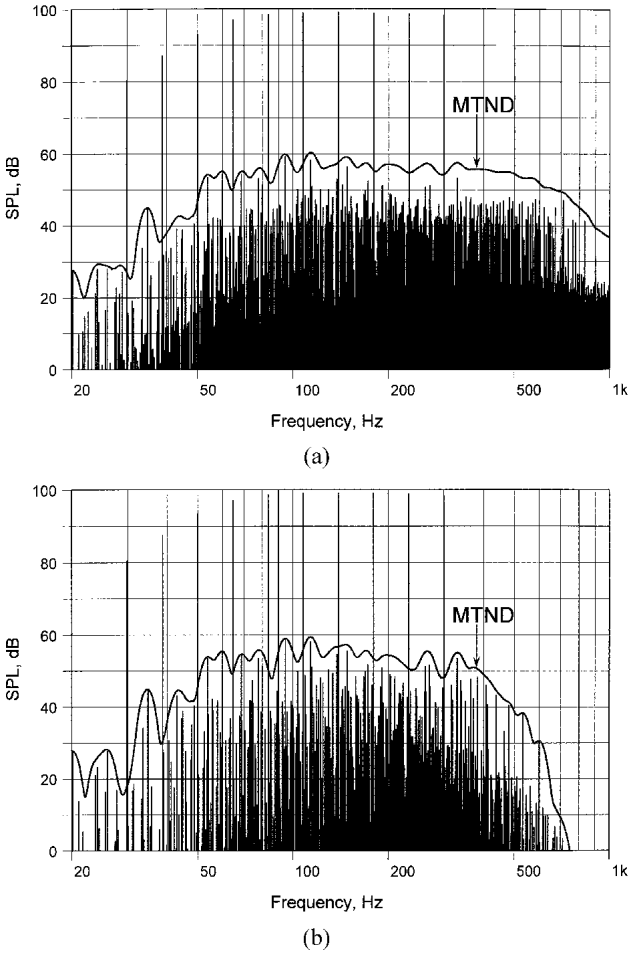

Fig. 18. Multitone reaction and MTND (solid curve) of 12-in (305-mm) woofer. (a) Nonlinearity is produced by *Bl* product, suspension stiffness, voice-coil inductance, and flux modulation. Input voltage $U = 3.3$ V; $X_{\max} = 2.5$ mm. (b) Same as (a), but flux modulation not taken into account.

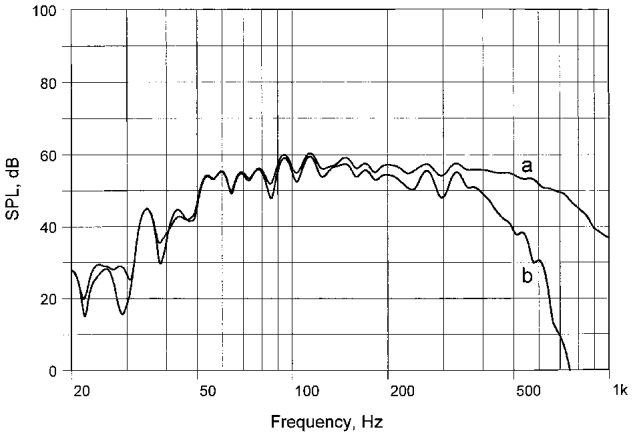

Fig. 19. SPL MTND corresponding to 12-in (305-mm) woofer. $U = 3.3$ *V;* $X_{\max} = 2.5$ mm. a—flux modulation taken into account; b—flux modulation omitted.

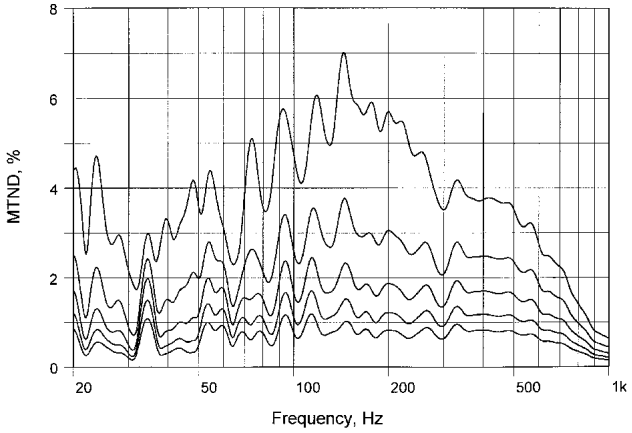

Fig. 20. MTND of 12-in (305-mm) woofer corresponding to increasing level of input voltage. $U_{\min} = 3.3$ V; voltage increments 3 dB.

handled through the use of the polynomial Vandermonde matrix [28], [33], which is not a trivial procedure. The separation of low-order and high-order distortion components can be performed easily by, for example, a two-tone signal. This is important for the detection of loudspeaker defects (rub and buzz) separate from regular motor and suspension nonlinearities. The simplicity of the distorted two-tone signal allows one to "understand" the relationship between some of the loudspeaker nonlinear parameters (causes) and nonlinear distortion (symptoms).

3.6 Coherence and Incoherence Functions

The next method that deserves discussion is the measurement of the coherence function that characterizes the degree of linear relationship between input and output as a function of frequency. By definition, the coherence function is expressed as the ratio of the square of the cross spectrum (between input and output) to the product of the autospectra of input and output [35],

$$\gamma^2(f_i) = \frac{|G_{xy}(f_i)|^2}{G_{xx}(f_i)G_{yy}(f_i)} \tag{17}$$

where $G_{xx}(f_i)$ is the autospectrum of the input signal $x(t)$ at the frequency f_i, $G_{yy}(f_i)$ is the autospectrum of the output signal $y(t)$, and $G_{xy}(f_i)$ is the cross spectrum of the input signal $x(t)$ and the output signal $y(t)$.

The functions $G_{xx}(f_i)$, $G_{yy}(f_i)$, and $G_{xy}(f_i)$ are calculated as follows:

$$G_{xx}(f_i) = E[X(f_i)\, X^*(f_i)] = \lim_{N\to\infty} \frac{1}{N}\sum_{n=1}^{N} X_n(f_i)\, X_n^*(f_i) \tag{18}$$

$$G_{yy}(f_i) = E[Y(f_i)\, Y^*(f_i)] = \lim_{N\to\infty} \frac{1}{N}\sum_{n=1}^{N} Y_n(f_i)\, Y_n^*(f_i) \tag{19}$$

$$G_{xy}(f_i) = E[X(f_i)\, Y^*(f_i)] = \lim_{N\to\infty} \frac{1}{N}\sum_{n=1}^{N} X_n(f_i)\, Y_n^*(f_i) \tag{20}$$

where * denotes complex conjugation, E indicates averaging, and $X(f)$ and $Y(f)$ are the complex spectra of the input and output signals $x(t)$ and $y(t)$, respectively,

$$X(f) = F\{x(t)\} = \int_{-\infty}^{\infty} x(t)\mathrm{e}^{-\mathrm{j}2\pi ft}\,\mathrm{d}t \tag{21}$$

$$Y(f) = F\{y(t)\} = \int_{-\infty}^{\infty} y(t)\mathrm{e}^{-\mathrm{j}2\pi ft}\,\mathrm{d}t \tag{22}$$

with $F\{\cdot\}$ being the Fourier transform.

In a strictly linear noiseless system the coherence function $\gamma^2(f)$ equals unity at all frequencies. To the contrary, if the input $x(t)$ and the output $y(t)$ have no relation to each other, the coherence function is zero. If the coherence function has a value between 0 and 1, the system under test may either be impaired by the nonlinear distortion or the noise, or both, or the output $y(t)$ depends on some other input processes along with $x(t)$. Therefore the coherence function may be used as a measure of nonlinearity in a device under test.

Historically use of the coherence function has never been immensely popular in loudspeaker testing. Meanwhile this method has found an application in the assessment of nonlinearity in hearing aids [3], [4]. The coherence function gives an integral lumped measure of the nonlinearity in a device under test, but it also takes into account noise if it is presented in a device under test. In loudspeaker testing the presence of noise does not seem to be an impeding factor. The attractive feature of the coherence function is its simple graphic representation. Plotting the set of coherence functions corresponding to different input levels is another nice option.

It seems to be more convenient to present the coherence function in the following manner and call it the incoherence function,

$$I(f) = \sqrt{1-\gamma^2(f)} \times 100(\%). \tag{23}$$

Expressed in percent, the incoherence function $I(f)$ is intuitively close to the concept of nonlinear distortion. Zero incoherence indicates the absence of nonlinear distortion and noise. There is a seeming similarity between the incoherence function and THD. However, there is a principal difference between these two characteristics. THD takes only harmonics into account, whereas the incoherence function is sensitive to the overall nonlinear contamination of the output signal and noise.

Fig. 21 shows the incoherence function of the 12-in (305-mm) woofer corresponding to different levels of the input signal. The initial level of the noise signal was 0.6 V rms. This level produced a voice-coil peak displacement of 2.5 mm. The same peak displacement corresponded to 10 V rms set for the measurement of THD SPL (see Fig. 8), and to 3.3 V rms for the multitone measurement (see Fig. 20). This difference in initial rms levels is attributed to different crest factors of these signals. The incoherence function, THD, and MTND each show a different pattern of nonlinear distortion. Due to the different nature of these three methods, they produce different data, all related to the same particular nonlinearity. This example demonstrates the complexity of assessment of nonlinear effects and the nontrivial reactions of a nonlinear system to different testing signals. Fig. 22 shows the difference between the incoherence functions of two 8-in (203-mm) woofers corresponding to voice-coil displacement of 4 and

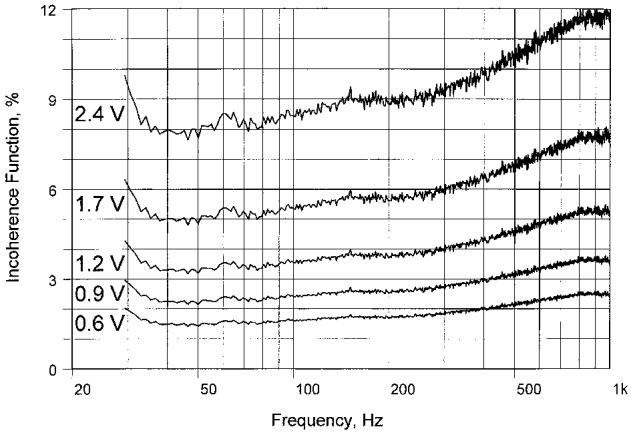

Fig. 21. Sound pressure incoherence function of 12-in (305-mm) woofer corresponding to increasing level of input voltage. $U_{\min}$ = 0.6 V; voltage increments 3 dB.

10 mm. An increase in the nonlinear distortion corresponding to the increasing input signal can be observed.

The incoherence function was calculated by means of the noise signal generated as a multitone signal with 4096 frequency components of equal amplitude and the random distribution of phases. The sampling frequency was 7680 Hz. The crest factor of this signal is 5.9. To adjust the properties of this noise signal for the numerical integration of the system of nonlinear differential equations governing the operation of a loudspeaker, an adaptive algorithm was used to provide the initial zero value of the testing signal. In the given examples the incoherence function resulted from 1000 averages, which would correspond to approximately 500 seconds of testing time. During this time the warming of the voice coil would change the behavior of the loudspeaker significantly if the driver were operated at high amplitudes. This is a drawback of this technique.

4 CONCLUSION

Due to the complex nature of loudspeaker nonlinearity and the intricacy of the human auditory system's reaction to musical signals contaminated with nonlinear distortion products, there are no undisputedly credible and commonly recognized thresholds of traditional nonlinear distortion measures related to the perceived sound quality. Since the dynamic reaction of a complex nonlinear system such as a loudspeaker cannot be extrapolated from its reaction to simple testing signals, such as a sweeping tone, the thresholds expressed in terms of the loudspeaker reaction to these signals (THD, harmonics, and two-tone intermodulation distortion) may not be valid.

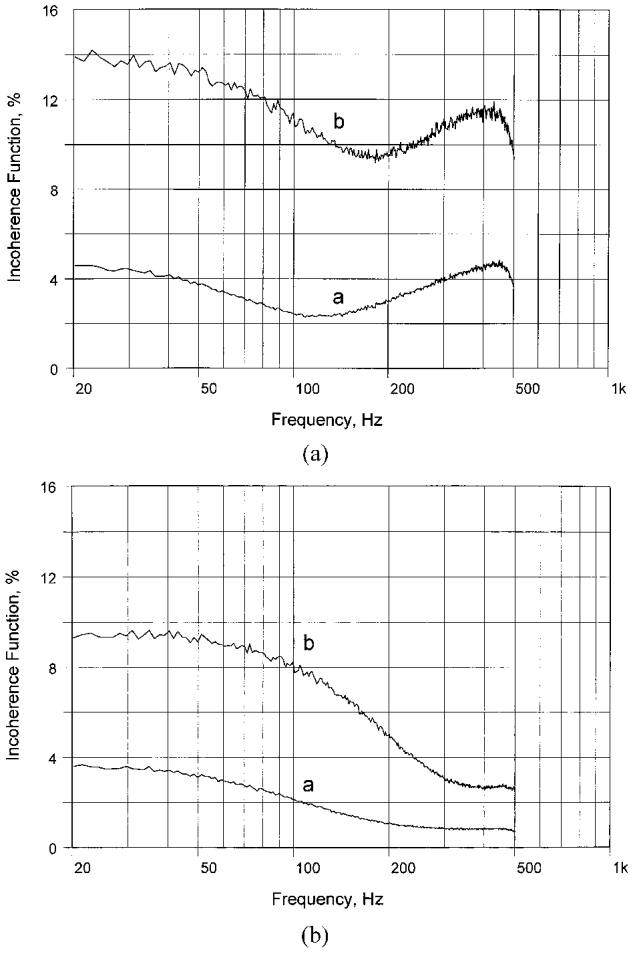

Fig. 22. Sound pressure incoherence function. a—peak level of input signal corresponds to $X_{max} = 4$ mm; b—peak level of input signal corresponds to $X_{max} = 10$ mm. (a) Loudspeaker A (long coil, short gap). (b) Loudspeaker B (short coil, long gap).

The requirements for an optimal method of measuring nonlinear distortion in loudspeakers were formulated. The optimal method to measure the nonlinearity in loudspeakers must be informative, that is, it must obtain enough objective information about the nonlinearity of different orders. The plotted measurement results must have a clear interpretation and be readily comprehensible. The measurement data must be supported psychoacoustically, meaning that there should exist an unambiguous relationship between the results presented and the expected sound quality.

In nonlinear systems such as a loudspeaker, the intermodulation distortion outweighs the harmonic distortion if a musical signal is reproduced. Harmonics may not give a quantitative measure of the nonlinear distortion in a loudspeaker, especially in the context of nonlinear distortion audibility. Nevertheless, the harmonic distortion measurement provides valuable information, illustrating, for example, the dominance of the nonlinearity of certain orders. A wide spectrum of harmonics and a strong level of high-order harmonics may be indicative of a loudspeaker malfunction such as a rubbing voice coil.

It has been demonstrated that high orders of static nonlinearity are characterized by a significant difference between the harmonic and intermodulation products that outnumber the harmonics and outweigh them in power. It has also been demonstrated that a high-order nonlinearity produces intermodulation and harmonic products of its "own" order, and of lower orders as well. The latter might have higher levels. Drawing the conclusion that a certain high-order nonlinearity is not essential because it produces a low level of its "own" harmonics may lead to wrong results.

THD does not seem to be a good measure of psychoacoustically meaningful distortion in loudspeakers. Not distinguishing different orders of harmonics, the THD frequency response may lead to the wrong conclusions about the performance of a loudspeaker. Similar levels of THD may correspond to very different distributions of harmonics of different orders. This difference, invisible to THD, may correspond to a strong diversity in intermodulation products and correspondingly significant differences in sound quality. However, THD can be legitimately used in testing where similar types of loudspeaker are compared (for example, in production testing).

Multitone testing possesses a number of advantages compared to other methods. It is fast and gives a detailed graphical representation of the distortion products. When a large number of input tones are applied to a loudspeaker, the spectrum of the output signal becomes very rich with intermodulation products (harmonic products have only a minuscule share of these spectral components). A visual examination of such a spectrum, though, may be difficult.

To circumvent this problem, the spectral components of different orders can be plotted separately. The separation of products of different orders needs postprocessing. Another option to simplify the visual interpretation of measurement results is to plot the average level of distortion confined within adjacent tones or to plot the level of the distortion products averaged in a sweeping frequency window. The comparatively high crest factor of multitone signals may give a "pessimistic" evaluation of the distortion level, registering the low-probability high-level peaks that may not be psychoacoustically relevant when a testing signal is replaced by a musical one. More research is required to put a reliable bridge between a loudspeaker's response to multitone stimuli and the sound quality of the loudspeaker. The results of recently published psychoacoustical research of a correlation between the responses to multitone stimuli and the audibility of distortion [26] imply that such a goal might possibly be reached.

The incoherence functions of two 8-in (203-mm) woofers were modeled at two different levels of the input noise signal. In addition, the incoherence function of a 12-in (305-mm) woofer was modeled for different levels of input signal. The incoherence function detected the difference in performance of the two motors, showing an increase in the overall nonlinear distortion for a loudspeaker having stronger voice-coil inductance modulation and stronger dependence of the *Bl* product on the voice-coil displacement.

There is a significant difference between THD, incoherence function, and reaction to multitone stimuli. All three methods provide an "integral" assessment of nonlinear distortion. However, the information conveyed by these methods is principally different. THD characterizes only harmonic distortion, omitting the intermodulation products, which significantly outweigh harmonics in a distorted musical signal. The incoherence function expressed in percent may be interpreted as a measure of the "lack of similarity" between the reference and the output signal. Contrary to THD, the incoherence function takes into account all nonlinear transformations of the signal as well as the influence of noise. However, this function does not distinguish the products of different orders, giving a "lumped" integral measure. The multitone stimulus provides information about harmonic and intermodulation products of various orders, but does it in a more diversified manner, making it possible to distinguish and analyze individual nonlinear products of different orders. The MTND response simplifies the interpretation of the nonlinear reaction to multitone stimuli by merging the numerous individual distortion spectral components into a single frequency response of distortion.

Measurement of the frequency-domain Volterra kernels is also discussed. Plotting these three-dimensional graphs of distortion of the second and third order is only feasible if a loudspeaker is characterized by a small level of distortion (weak nonlinearity). This method quickly loses its accuracy if the level of distortion is high. High-order Volterra kernels do not have a readily comprehensible graphical representation.

Of all the methods surveyed and simulated, multitone testing seems to be the most feasible in the context of distortion audibility for the assessment of loudspeaker large-signal performance and nonlinearity measurements. Nevertheless, harmonic and the traditional two-tone intermodulation distortion should not be withdrawn from the list of standard characteristics. THD is a lower resolution measure of nonlinearity, but can still be used for the comparison of loudspeakers of the same type. Multitone testing is good for both intermodulation distortion measurements and the maximum SPL check. For the latter the multitone burst should be used. In addition, multitone testing is good for loudspeaker quality control testing.

Setting any boundaries relating objective information and nonlinear distortion audibility requires extensive computer simulation and involved psychoacoustical tests. Without such information about the relationship between objective and subjective parameters, the measurement data will only be able to tell us that one loudspeaker has more or less nonlinear distortion. The question of how critical this difference is from the standpoint of distortion audibility will remain unanswered.

5 REFERENCES

[1] E. Czerwinski, A. Voishvillo, S. Alexandrov, and A. Terekhov, "Multitone Testing of Sound System Components—Some Results and Conclusions, Part 1: History and Theory," *J. Audio Eng. Soc.,* vol. 49, pp. 1011–1048 (2001 Nov.); "Multitone Testing of Sound System Components—Some Results and Conclusions, Part 2: Modeling and Application," ibid., pp. 1181–1192 (2001 Dec.).

[2] N. Wiener, *Nonlinear Problems in Random Theory* (Technology Press, M.I.T., and Wiley, New York, 1958).

[3] O. Dyrlund, "Characterization of Nonlinear Distortion in Hearing Aids Using Coherence Function," *Scand. Audiol.,* vol. 18, pp. 143–148 (1989).

[4] J. Kates, "On Using Coherence to Measure Distortion in Hearing Aids," *J. Acoust. Soc. Am.,* vol. 91, pt.1, pp. 2236–2244 (1992 Apr.).

[5] Y. Cho, S. Kim, E. Hixson, and E. Powers, "A Digital Technique to Estimate Second-Order Distortion Using Higher Order Coherence Spectra," *IEEE Trans. Signal Process.,* vol. 40, pp. 1029–1040 (1992 May).

[6] U. Totzek and D. Preis, "How to Measure and Interpret Coherence Loss in Magnetic Recording," *J. Audio Eng. Soc.,* vol. 35, pp. 869–887 (1987 Nov.).

[7] D. Jensen and G. Sokolich, "Spectral Contamination Measurements," presented at the 85th Convention of the Audio Engineering Society, *J. Audio Eng. Soc.* (*Abstracts*), vol. 36, p. 1034 (1988 Dec.), preprint 2725.

[8] R. C. Cabot, "Fast Response and Distortion Testing," presented at the 90th Convention of the Audio Engineering Society, *J. Audio Eng. Soc.* (*Abstracts*), vol. 39, p. 385 (1991 May), preprint 3045.

[9] R. Metzler, "Test and Calibration Application of Multitone Signals," in *Proc AES 11th Int. Conf.* (1992 May), pp. 29–36.

[10] J. Vanderkooy and S. G. Norcross, "Multitone Testing of Audio Systems," presented at the 101st Con-

vention of the Audio Engineering Society, *J. Audio Eng. Soc.* (*Abstracts*), vol. 44, p. 1174 (1996 Dec.), preprint 4378.

[11] P. Schweizer, "Feasibility of Audio Performance Using Multitones," in *Proc. AES UK Conf. on the Measure of Audio* (1997 Apr.), pp. 34–40.

[12] J. M. Risch, "A New Class of In-Band Multitone Test Signals," presented at the 105th Convention of the Audio Engineering Society, *J. Audio Eng. Soc.* (*Abstracts*), vol. 46, p. 1037 (1998 Nov.), preprint 4803.

[13] V. Volterra, *Theory of Functionals and of Integral and Integrodifferential Equations* (Dover, New York, 1959).

[14] M. Schetzen, *Volterra and Wiener Theories of Nonlinear Systems* (Krieger Publ., Malabar, FL, 1989).

[15] A. M. Kaizer, "Modeling of the Nonlinear Response of an Electrodynamic Loudspeaker by a Volterra Series Expansion," *J. Audio Eng. Soc.,* vol. 35, pp. 421–433 (1987 June).

[16] M. J. Reed and M. O. Hawksford, "Practical Modeling of Nonlinear Audio Systems Using the Volterra Series," presented at the 100th Convention of the Audio Engineering Society, *J. Audio Eng. Soc.* (*Abstracts*), vol. 44, pp. 649–650 (1996 July/Aug.), preprint 4264.

[17] M. J. Reed and M. O. J. Hawksford, "Comparison of Audio System Nonlinear Performance in Volterra Space," presented at the 103rd Convention of the Audio Engineering Society, *J. Audio Eng. Soc.* (*Abstracts*), vol. 45, p. 1026 (1997 Nov.), preprint 4606.

[18] G. Cibelli, E. Ugolotti, and A. Bellini, "Dynamic Measurements of Low-Frequency Loudspeakers Modeled by Volterra Series," presented at the 106th Convention of the Audio Engineering Society, *J. Audio Eng. Soc.* (*Abstracts*), vol. 47, p. 534 (1999 June), preprint 4968.

[19] J. Hilliard, "Distortion Tests by the Intermodulation Method," *Proc. IRE,* vol. 29, pp. 614–620 (1941 Dec.).

[20] H. Scott, "The Measurement of Audio Distortion," *Communications,* pp. 25–32, 52–56 (1946 Apr.).

[21] AES2-1984 (r. 2003), "AES Recommended Practice—Specification of Loudspeaker Components Used in Professional Audio and Sound Reinforcement," Audio Engineering Society, New York (2003).

[22] IEC 60268-5, "Sound System Equipment—Part 5 Loudspeakers," International Electrotechnical Commission, Geneva, Switzerland (2000).

[23] D. Keele, "Method to Measure Intermodulation Distortion in Loudspeakers," proposals for the working group SC-04-03-C, Audio Engineering Society, New York (2000).

[24] D. B. Keele, "Development of Test Signals for the EIA-426-B Loudspeaker Power-Rating Compact Disk," presented at the 111th Convention of the Audio Engineering Society, *J. Audio Eng. Soc.* (*Abstracts*), vol. 49, p. 1224 (2001 Dec.), convention paper 5451.

[25] E. Zwicker, H. Fastl, and H. Frater, *Psychoacoustics: Facts and Models,* Springer ser. in Information Sciences, 2nd updated ed. (Springer, New York, 1999).

[26] C. T. Tan, B. C. J. Moore, and N. Zacharov, "The Effect of Nonlinear Distortion on the Perceived Quality of Music and Speech Signals," *J. Audio Eng. Soc.,* vol. 51, pp. 1012–1031 (2003 Nov.).

[27] M. Reed and M. Hawksford, "Identification of Discrete Volterra Series Using Maximum Length Sequences," *IEEE Proc. Circuits Dev. Sys.,* vol. 143, pp. 241–248 (1996 Oct.).

[28] S. Boyd, Y. Tang, and L. Chua, "Measuring Volterra Kernels," *IEEE Trans. Circuits Sys.,* vol. CAS-30, pp. 571–577 (1983 Aug.).

[29] R. Nowak and B. Van Veen, "Random and Pseudorandom Inputs for Volterra Filter Identification," *IEEE Trans. Signal Process.,* vol. 42, pp. 2124–2135 (1994 Aug.).

[30] H. K. Jang and K. J. Kim, "Identification of Loudspeaker Nonlinearities Using the NARMAX Modeling Technique," *J. Audio Eng. Soc.,* vol. 42, pp. 50–59 (1994 Jan./Feb.).

[31] D. Shorter, "The Influence of High Order Products on Nonlinear Distortion," *Electron. Eng.,* vol. 22, pp. 152–153 (1950).

[32] E. Geddes, *Audio Transducers* (Geddlee, 2002), pp. 236–241.

[33] G. Golub and C. Van Loan, *Matrix Computations* (Johns Hopkins University Press, Baltimore, MD, 1996).

[34] A. Voishvillo, "Nonlinear Distortion in Professional Sound Systems—From Voice Coil to the Listener," presented at the Acoustical Conference of the Institute of Acoustics "Reproduced Sound 17" (Stratford-upon-Avon, UK, 2001 Nov. 16–18).

[35] J. Bendat and A. Piersol, *Random Data: Analysis and Measurement Procedures* (Wiley, New York, 1986).

APPENDIX 1

REFERENCE LOUDSPEAKERS

A1.1 12-in (305-mm) Woofer

The parameters of an experimental 12-in woofer were obtained from measurements by the Klippel analyzer. In addition, force factor modulation by the voice-coil current was modeled using FEM (Fig. 23). The small-signal (rest-

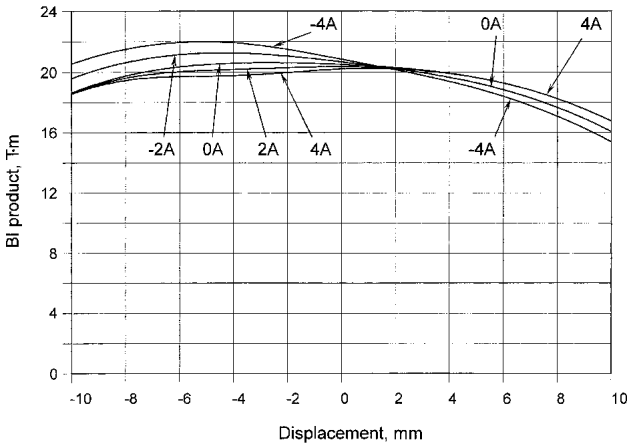

Fig. 23. *Bl* product affected by flux modulation. Experimental 12-in (305-mm) woofer with overhung voice coil. Coil diameter 75 mm; coil height 38 mm; top plate thickness 15 mm.

position) parameters of the 12-in woofer used in this work are given in Table 4. The length of the voice coil is 38 mm, the diameter is 75 mm, and the thickness of the top plate is 15 mm. The excursion-dependent parameters C_{ms}, K_{ms}, Bl, and L_1 are shown in Fig. 24. Distortions were simulated for the woofer placed in a sealed 40-liter box.

A1.2 Two 8-in (203-mm) Woofers

The two 8-in woofers used in the experiments and modeling have similar suspension and different motors (Fig. 25). One loudspeaker has a long coil (12 mm) and a short gap (6 mm), the other has a short coil (6 mm) and a long gap (12 mm) (Fig. 26). The diameter of both coils is 1.5 in

Table 4

Bl (T · m)	K_{ms} (N/mm)	C_{ms} (mm/N)	m_{ms} (g)	R_{ms} (kg/s)	R_e (Ω)	R_2 (Ω)	L_e (mH)	L_2 (mH)	f_s (Hz)	Q_{es}	Q_{ms}	Q_{ts}	V_{as} (dm^3)
20.5	6.55	0.15	232	2.82	5.22	10.4	2.46	1.28	26.8	0.48	13.8	0.46	335

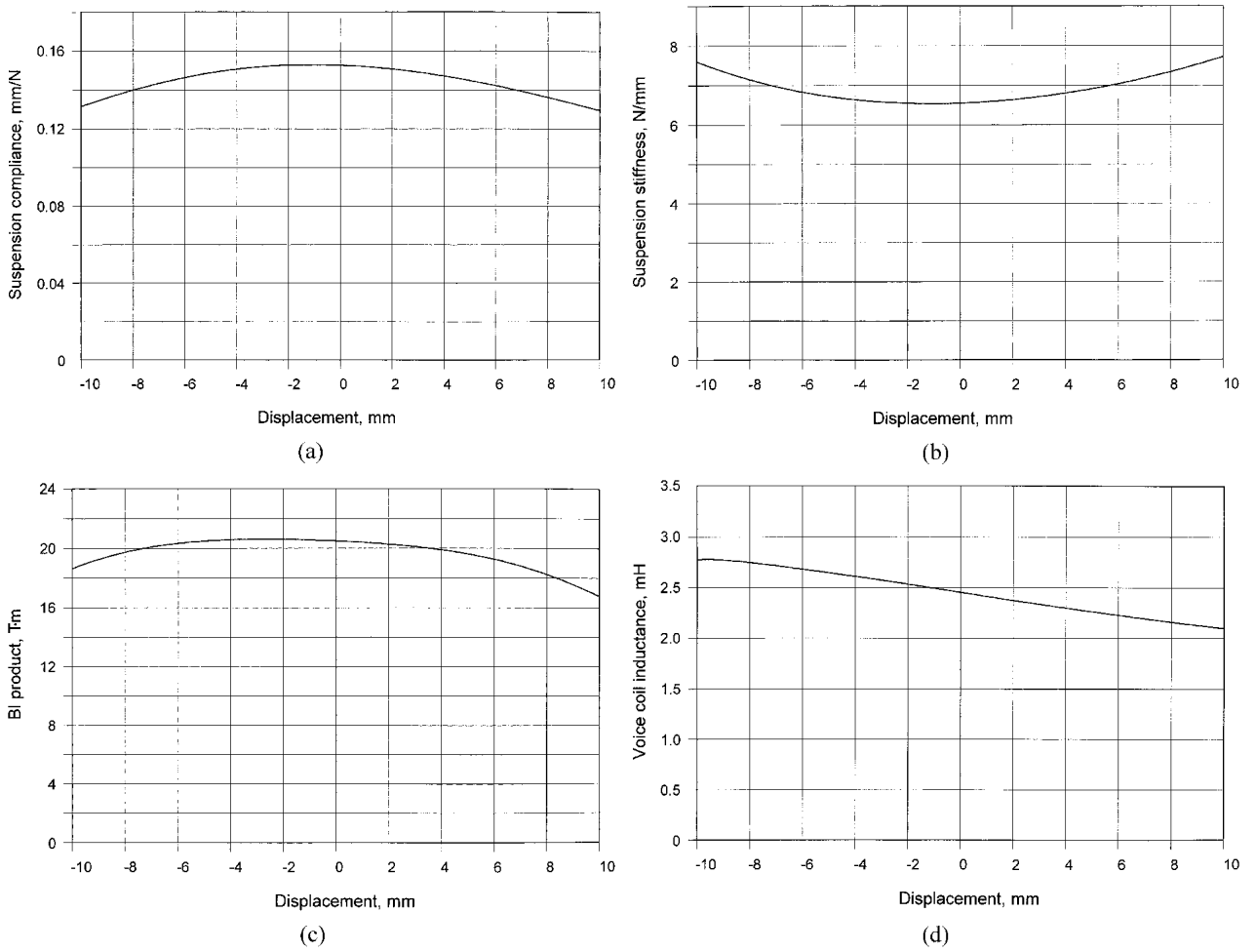

Fig. 24. Excursion-dependent parameters of 12-in (305-mm woofer. (a) Suspension compliance. (b) Suspension stiffness. (c) Bl product. (d) Voice-coil inductance.

Fig. 25. Reference 8-in (203-mm) woofers used in experiments and modeling. (a) Loudspeaker A [long coil (12 mm), short gap (6 mm)]. (b) Loudspeaker B [short coil (6 mm), long gap (12 mm)].

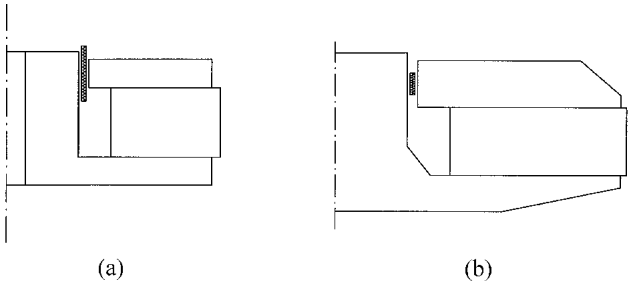

Fig. 26. Rest positions of voice coils in gap. (a) Loudspeaker A (long coil, short gap). (b) Loudspeaker B (short coil, long gap).

(38 mm). Both loudspeakers did not have dust caps to prevent any possible artifacts caused by the compression of the air underneath a dust cap or distortion due to the turbulent airflow in a pole piece vent. The small-signal (rest-position) parameters of the loudspeakers are listed in Table 5.

The nonlinear displacement-dependent parameters for loudspeaker A are given in Fig. 27, those for loudspeaker B in Fig. 28. Loudspeaker A (long coil, short gap) has stronger overall variations of the *Bl* product and voice-coil inductance. Using the criterion of the maximum displacement X_{max} corresponding to a decrease in the suspension compliance $C_{ms}(x)$ to 0.12 mm/N, which is to 30% of its initial value of 0.41 mm/N, the X_{max} values of both loudspeakers were set to 10 mm. At this displacement the *Bl* product in loudspeaker A is 2.0 T · m, which is 22% of its initial value of 9.0 T · m. The *Bl* product of the second driver drops to 3.5 T · m, which is 47% of its resting position value of 7.5 T · m. Such a comparatively moderate decrease in the *Bl* product for loudspeaker B is explained by the use of an underhung voice coil.

Using similar suspensions in both loudspeakers and setting identical values of $X_{max} = 10$ mm helped to compare the difference in nonlinear distortion in these loudspeakers caused by the difference in motor parameters.

Table 5

Loudspeaker	*Bl* (T · m)	K_{ms} (N/mm)	C_{ms} (mm/N)	m_{ms} (g)	R_{ms} (kg/s)	R_e (Ω)	R_2 (Ω)	L_e (mH)	L_2 (mH)	f_s (Hz)	Q_{es}	Q_{ms}	Q_{ts}	V_{as} (dm^3)
A Long coil, short gap	9.0	2.44	0.41	19.2	1.5	5.5	5.4	0.72	0.38	57	0.46	4.6	0.42	33
B Short coil, long gap	7.5	2.44	0.41	16.0	1.5	5.3	2.4	0.56	0.29	62	0.60	4.2	0.52	33

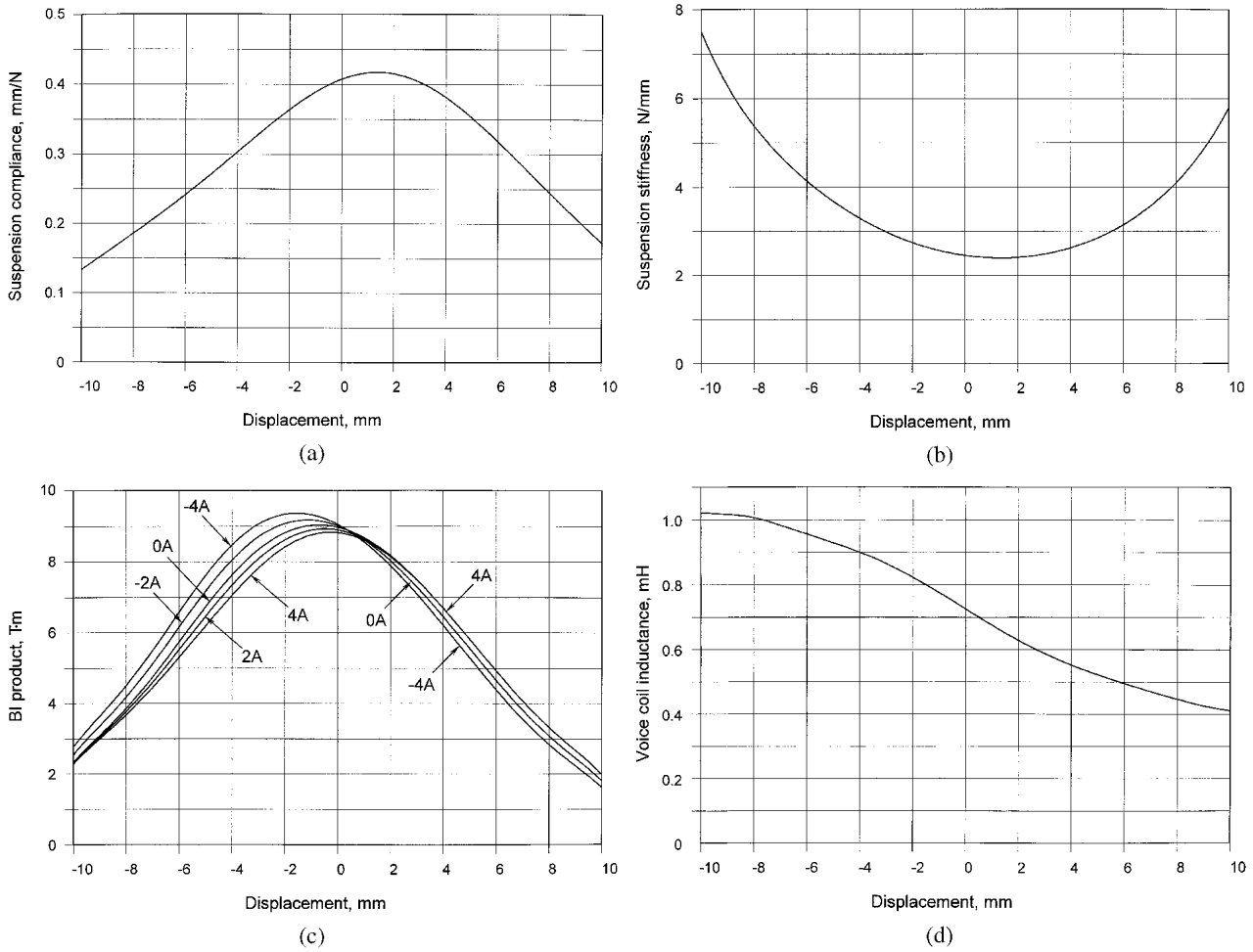

Fig. 27. Parameters of loudspeaker A (long coil, short gap) as a function of voice-coil displacement. (a) Suspension compliance. (b) Suspension stiffness. (c) *Bl* product; current increments 2 A. (d) Voice-coil inductance.

APPENDIX 2

LOUDSPEAKER NONLINEAR MODEL

The nonlinear behavior of the reference loudspeakers was researched numerically using the model described by a system of two nonlinear differential equations,

$$U = R_e i + \frac{d\Phi_1(x,\,t)}{dt} + \frac{d\Phi_2(x,\,t)}{dt} + [Bl(x) + \Delta Bl(x,\,i)]\frac{dx}{dt} \tag{24}$$

$$[Bl(x) + \Delta Bl(x,\,i)]i - \frac{dL_e(x)}{dx}\frac{i^2}{2} - \frac{dL_2(x)}{dx}\frac{i_2^2}{2} = \frac{d^2x}{dt^2}m_{ms} + \frac{dx}{dt}R_{ms} + xK_{ms}(x) \tag{25}$$

where U is the input voltage, i is the voice-coil current, R_e is the voice-coil resistance, x is the voice-coil excursion, $\Phi_1(x,\,t)$ is the alternating magnetic flux related to the voice-coil inductance $L_e(x)$, $\Phi_2(x,\,t)$ is the alternating flux related to the parainductance $L_2(x)$, $Bl(x)$ is the force product, $\Delta Bl(x,\,i)$ is the function responsible for the modulation of the flux, induction, and $Bl(x)$ product of the gap, i_2 is the current through the parainductance $L_2(x)$, m_{ms} is the moving mass of the diaphragm and voice coil, R_{ms} denotes the mechanical losses in the suspension, and $K_{ms}(x)$ is the suspension stiffness.

The terms

$$\frac{dL_e(x)}{dx}\frac{i^2}{2} \quad \text{and} \quad \frac{dL_2(x)}{dx}\frac{i_2^2}{2}$$

are the reluctance forces produced by the voice-coil inductance $L_e(x)$ and the parainductance $L_2(x)$. The time derivatives of the alternating fluxes $\Phi_1(x,\,t)$ and $\Phi_2(x,\,t)$ are expressed as

$$\frac{d\Phi_1(x,\,t)}{dt} = L_e(x)\frac{di}{dt} + \frac{dL_e(x)}{dx}\frac{dx}{dt}i \tag{26}$$

$$\frac{d\Phi_2(x,\,t)}{dt} = L_2(x)\frac{di_2}{dt} + \frac{dL_2(x)}{dx}\frac{dx}{dt}i_2. \tag{27}$$

The sound pressure response was calculated by the simple far-field half-space expression

$$p(t) = \frac{dy(t)}{dt}\frac{S_{eff}\rho}{2\pi r} \tag{28}$$

where $y(t)$ is the voice-coil velocity, $dy(t)/dt$ is the voice-coil acceleration, S_{eff} is the diaphragm effective area, ρ is the air density, and r is the distance from the diaphragm to the observation point.

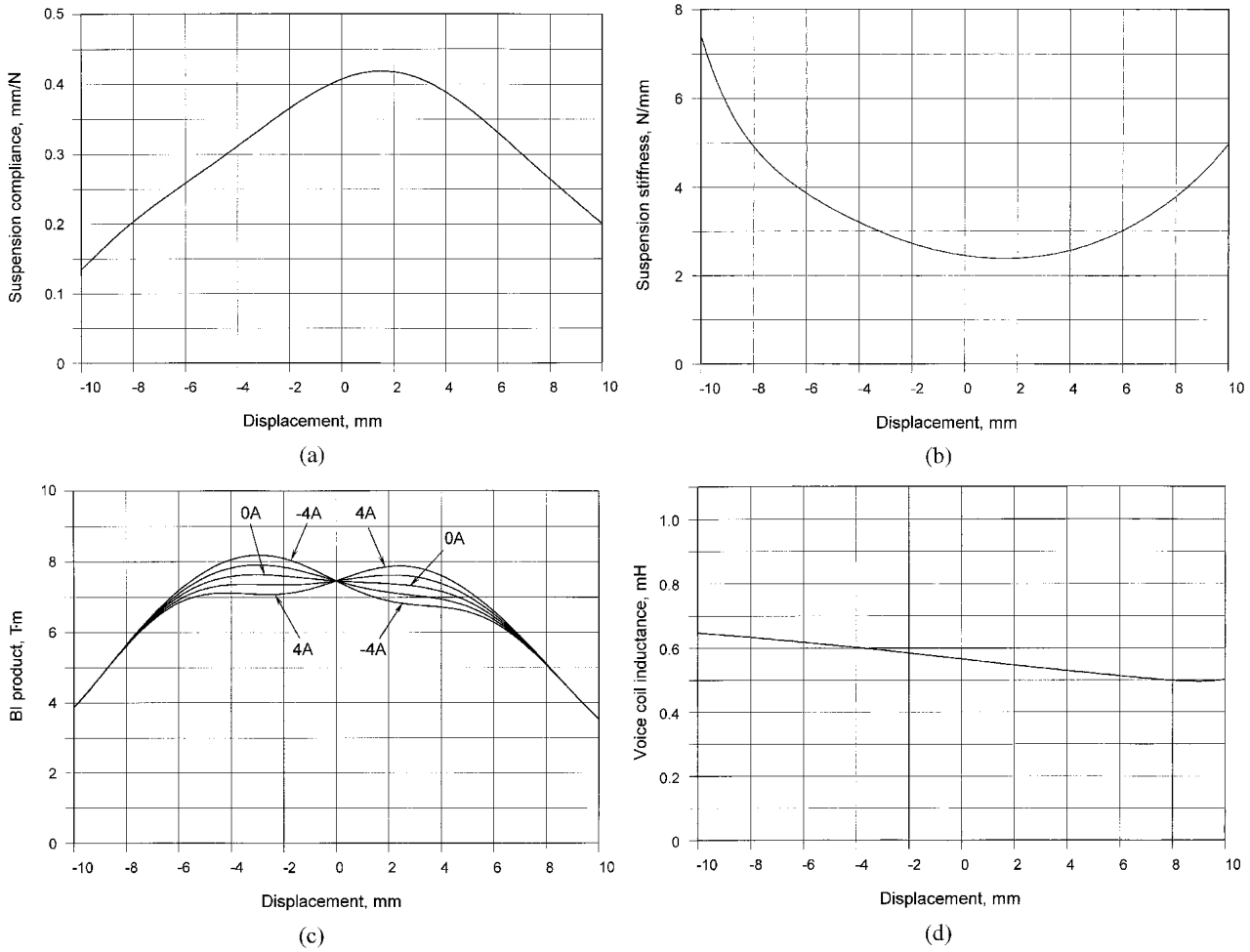

Fig. 28. Parameters of loudspeaker B (short coil, long gap) as a function of voice-coil displacement. (a) Suspension compliance. (b) Suspension stiffness. (c) *Bl* product; current increments 2 A. (d) Voice-coil inductance.

The system of Eqs. (24), (25) was transformed into the canonical Cauchy form and solved numerically by the classical Runge–Kutta method of the fourth order. The vector form of the state variables is

$$\boldsymbol{Z}(t) = \{z_1(t), z_2(t), z_3(t), z_4(t)\}^{\mathrm{T}} \tag{29}$$

$$\boldsymbol{\Phi}(t, \boldsymbol{Z}) = \{\varphi_1(t, \boldsymbol{Z}), \varphi_2(t, \boldsymbol{Z}), \varphi_3(t, \boldsymbol{Z}), \varphi_4(t, \boldsymbol{Z})\} \tag{30}$$

where $z_1(t)$ denotes the current $i_2(t)$ in the parainductance $L_2(x)$, $z_2(t)$ stands for the voice-coil current i, $z_3(t)$ accounts for the voice-coil displacement $x(t)$, $z_4(t)$ is the voice-coil velocity $\mathrm{d}x(t)/\mathrm{d}t$, and $\boldsymbol{\Phi}(t, \boldsymbol{Z})$, is the vector formulation of the derivatives of the current $\mathrm{d}i_2(t)/\mathrm{d}t$, the derivative of the voice-coil current $\mathrm{d}i(t)/\mathrm{d}t$, the voice-coil velocity $y(t)$, and the voice-coil acceleration $\mathrm{d}y(t)/\mathrm{d}t$.

The Cauchy vector form of the system of Eqs. (24), (25) and the initial conditions are

$$\begin{aligned} &\frac{\mathrm{d}\boldsymbol{Z}(t)}{\mathrm{d}t} = \boldsymbol{\Phi}[t, \boldsymbol{Z}(t)] \\ &\boldsymbol{Z}(t_0) = \boldsymbol{Z}_0. \end{aligned} \tag{31}$$

The integration steps are carried out according to the following algorithm:

$$\boldsymbol{Z}_{n+1} = \boldsymbol{Z}_n + h\boldsymbol{K}_n \tag{32}$$

$$\boldsymbol{K}_n = \frac{1}{6}(\boldsymbol{K}_n^{(1)} + 2\boldsymbol{K}_n^{(2)} + 2\boldsymbol{K}_n^{(3)} + \boldsymbol{K}_n^{(4)}) \tag{33}$$

and

$$\begin{aligned} &\boldsymbol{K}_n^{(1)} = \boldsymbol{\Phi}(t_n, \boldsymbol{Z}_n) \\ &\boldsymbol{K}_n^{(2)} = \boldsymbol{\Phi}\left(t_n + \frac{h}{2}, \boldsymbol{Z}_n + \frac{h}{2}\boldsymbol{K}_n^{(1)}\right) \\ &\boldsymbol{K}_n^{(3)} = \boldsymbol{\Phi}\left(t_n + \frac{h}{2}, \boldsymbol{Z}_n + \frac{h}{2}\boldsymbol{K}_n^{(2)}\right) \\ &\boldsymbol{K}_n^{(4)} = \boldsymbol{\Phi}(t_n + h, \boldsymbol{Z}_n + h\boldsymbol{K}_n^{(3)}) \end{aligned} \tag{34}$$

where h is the time increment.

The vector

$$\frac{\mathrm{d}\boldsymbol{Z}(t)}{\mathrm{d}t} = \left[\frac{\mathrm{d}\boldsymbol{Z}_1(t)}{\mathrm{d}t}, \frac{\mathrm{d}\boldsymbol{Z}_2(t)}{\mathrm{d}t}, \frac{\mathrm{d}\boldsymbol{Z}_3(t)}{\mathrm{d}t}, \frac{\mathrm{d}\boldsymbol{Z}_4(t)}{\mathrm{d}t}\right]^{\mathrm{T}}$$

is expressed through the loudspeaker parameters as

$$\begin{aligned} &\frac{\mathrm{d}\boldsymbol{Z}_1(t)}{\mathrm{d}t} = \frac{\mathrm{d}i_2}{\mathrm{d}t} = \frac{1}{L_2(x)}\left\{R_2(x)i - i_2\left[R_2(x) - \frac{\mathrm{d}L_2(x)}{\mathrm{d}x}\frac{\mathrm{d}x}{\mathrm{d}t}\right]\right\} \\ &\frac{\mathrm{d}\boldsymbol{Z}_2(t)}{\mathrm{d}t} = \frac{\mathrm{d}i}{\mathrm{d}t} = \frac{1}{L_e(x)}\left[U - iR_e - i\frac{\mathrm{d}L_e(x)}{\mathrm{d}x}\frac{\mathrm{d}x}{\mathrm{d}t} - L_2(x)\frac{\mathrm{d}i_2}{\mathrm{d}t}\right. \\ &\qquad\left. - i_2\frac{\mathrm{d}L_2(x)}{\mathrm{d}x}\frac{\mathrm{d}x}{\mathrm{d}t} - Bl(x) - \Delta Bl(x, i)\right] \\ &\frac{\mathrm{d}\boldsymbol{Z}_3(t)}{\mathrm{d}t} = \frac{\mathrm{d}x}{\mathrm{d}t} = y \\ &\frac{\mathrm{d}\boldsymbol{Z}_4(t)}{\mathrm{d}t} = \frac{\mathrm{d}y}{\mathrm{d}t} = \frac{1}{m_{\mathrm{ms}}}\left\{[Bl(x) + \Delta Bl(x, i)]i - \frac{\mathrm{d}L_e(x)}{\mathrm{d}x}\frac{i^2}{2}\right. \\ &\qquad\left. - \frac{\mathrm{d}L_2(x)}{\mathrm{d}x}\frac{i_2^2}{2} - R_{\mathrm{ms}}y - K_{\mathrm{ms}}(x)x\right\}. \end{aligned} \tag{35}$$

The function $\Delta Bl(x, i)$ was calculated by the finite-element method (FEM). The FEM static model of magnet assembly was built and the model of the voice coil was incorporated. The voice-coil model was ascribed the geometrical dimensions, number of turns, and constant current. Using the quasi-dynamic approach, that is, assigning different values of voice-coil current (of positive and negative polarity), the distribution of the gap induction was calculated. This procedure was repeated a number of times for different positions of the voice coil. Afterward the Bl product was calculated for the corresponding discrete values of the voice-coil current $\pm I_a, \pm I_b \pm \cdots \pm I_m$ and the positions of the voice coil $\pm X_1, \pm X_2 \pm \cdots \pm X_n$. The function $\Delta Bl(x, i)$ approximated the variation of the Bl product caused by the voice-coil current.

The loudspeaker parameters were measured by the Klippel analyzer and incorporated into the model. Integration of the system of Eqs. (24), (25) was performed using different input signals to model different measurement conditions. The signal duration and sampling frequency were optimized for a particular signal. The sampling was linked to the time interval h used in the Runge–Kutta solution of the system (24), (25). The details of the solution are not discussed here because they do not have direct relation to the subject of this paper.

THE AUTHORS


A. Voishvillo


A. Terekhov

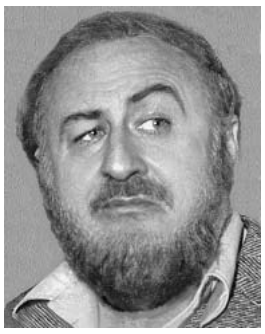
E. Czerwinski


S. Alexandrov

Alexander Voishvillo was born and raised in Leningrad (now Saint Petersburg), Russia. He received a Ph.D. degree in 1987 for work centered on computer optimization of loudspeaker crossover systems.

From 1977 to 1995 he worked at the Laboratory of Prospective Research and Development, Popov Institute for Radio and Acoustics, Saint Petersburg. While at the Popov Institute he designed loudspeaker systems for manufacturers and did research work on loudspeakers. He was responsible for the development of specialized studio monitors for the Russian Broadcasting Corporation. In 1995 he moved to California, accepting an invitation of Gene Czerwinski of Cerwin-Vega Inc., to head a new research and development group. His responsibilities included the development of new transducers, as well as research work on nonlinearity in sound systems and advanced methods of measurement of nonlinear distortion in audio equipment. He continued his collaboration with Gene Czerwinski at Cerwinski Labs, a new R&D company established in 2002, where he has been working on the development of original professional high-frequency transducers and on alternative methods of assessing nonlinearity in audio equipment.

Dr. Voishvillo holds several U.S. patents on new types of transducers. He is the author of more than 30 publications on loudspeakers, including the engineering book on loudspeaker theory and design, *High Quality Loudspeaker Systems and Transducers,* published in Russia in 1985 as well as several publications in the *Journal.* He is a member of the Audio Engineering Society and participates in a working group on loudspeaker measurements and modeling at the AES Standards Committee. He is also a member of the *JAES* Review Board.

●

Alexander Terekhov was born in Leningrad (now Saint Petersburg), Russia, in 1952. He received an M.Sc. degree in broadcasting and radio communication from the State University of Telecommunications in 1974.

From 1981 to 1991 he worked as a research associate in the Laboratory of Prospective Acoustic Research and Development at the Popov R&D Institute for Radio and Acoustics, Saint Petersburg. His activities included research on loudspeaker testing and measurements and binaural stereophony. In 1991 he joined Audion Ltd., Saint Petersburg, as a senior research associate and chief engineer. He came to the United States in 1996 and since 1997 has been employed as an acoustic research engineer at Cerwin-Vega, Inc., and subsequently at Czerwinski Laboratories. His professional activity is being focused on acoustic research, the development of new software for various R&D needs, including loudspeaker measurement systems, and research on air propagation distortion.

Mr. Terekhov has presented technical papers at Russian audio conventions and in recent years coauthored several papers on air propagation distortion published in the *Journal.*

●

Eugene Czerwinski studied electrical engineering at the University of Toledo, where he received a B.S.E.E. degree.

He worked as an associate professor of electronics at the University of Michigan Engineering Research Institute. Later he was a development engineer at Willys Motors Electronic Division, where he designed UHF TV transmitting equipment, studio cameras, and audio systems. In 1954 he joined the test division of Douglas Aircraft, where he designed measurement equipment, including a multichannel sound spectrum analyzer for jet engines. At his next job, with Bendex Pacific, he designed the first of its kind 10 000-watt germanium solid-state amplifier for sonar transducers.

His passion for music determined his future life and career. Coming from a musically deprived childhood, he was exposed to a live orchestral sound as a young man, which affected him profoundly. He wanted to be able to replicate this experience at his time of choosing. While at Bendex he established Vega Associates, which designed and manufactured custom high-fidelity systems. In 1973 it became Cerwin-Vega, Inc. He headed the company for the next three decades and developed the first quarter-kilowatt transistor audio amplifier and four-way 18-in loudspeaker system. In 1964 he started experimenting with live sound reinforcement for large-venue rock concerts. He worked with Universal Studios to develop the Sensurround system, which received an Academy Award in 1974 for special technical achievement in sound. Sensurround was used nationwide in cinemas to realistically simulate vibrations for the "Earthquake" movie, and was a precursor to the high-impact theater sound systems later developed by Lucas Sound and Dolby, Inc. His lifelong interest in music motivated Mr. Czerwinski to establish in 1989 a nonprofit recording company, the MAMA (Musical Archives, Musical Archives) Foundation. The Foundation's goal is to preserve the music of culturally significant artists whose music does not have broad commercial appeal. MAMA has released over 30 state-of-the-art digital recordings of jazz and big-band music, and garnered critical acclaim, including six Grammy nominations and two Grammy Awards. In 2003 he sold Cerwin-Vega and founded Cerwinski Laboratories, Inc. At Cerwinski Labs he continues important research into air-propagation distortion and multichannel sound reinforcement and reproduction.

Mr. Czerwinski has authored and coauthored numerous patents on loudspeakers (six patents are currently pending).

●

Sergei Alexandrov was born in Leningrad (now Saint Petersburg), Russia. He received an M.Sc. degree in electrical engineering from Leningrad University in 1979.

From 1969 to 1978 he worked as a development engineer at the Marine Equipment R&D Institute. From 1978 to 1991 he held a principal position in the R&D group at Popov R&D Institute for Radio and Acoustics, Saint Petersburg, where he developed power amplifiers and audio signal processors for high-fidelity and studio applications. In 1991 he cofounded and became president and CEO of Audion Ltd., Saint Petersburg, an audio electronics and loudspeaker test equipment manufacturing company. In 1996 he came to the United States and held a staff position as an acoustic R&D engineer at Cerwin-Vega, Inc., until 2002. There he developed original computer-controlled loudspeaker measurement systems, loudspeaker power testing devices, and a computer-based system for nonlinear distortion audibility research. He continued his collaboration with Gene Czerwinski (the founder of Cerwin-Vega) at Cerwinski Labs, where he has been working on loudspeaker magnet system field optimization and nonstandard test equipment design.

Mr. Alexandrov has presented a number of technical papers at Russian audio and electronics conventions. He has publications on homomorphic signal analysis, binaural stereophony, audio signal processing, and loudspeaker measurements to his credit and coauthored several publications in the *Journal.*